TOP 5 ORAL PRESENTATIONS

Clinical Prognostication in Acute Necrotizing Encephalopathy of Childhood: Role of MR Imaging Severity Assessment

Kiran Hilal

Department of Radiology, Aga Khan University Hospital, Karachi, Pakistan

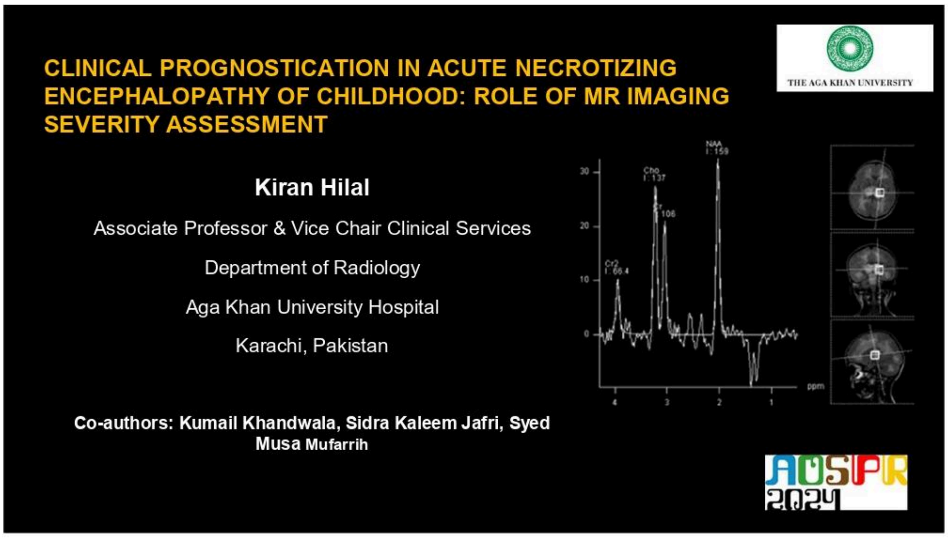

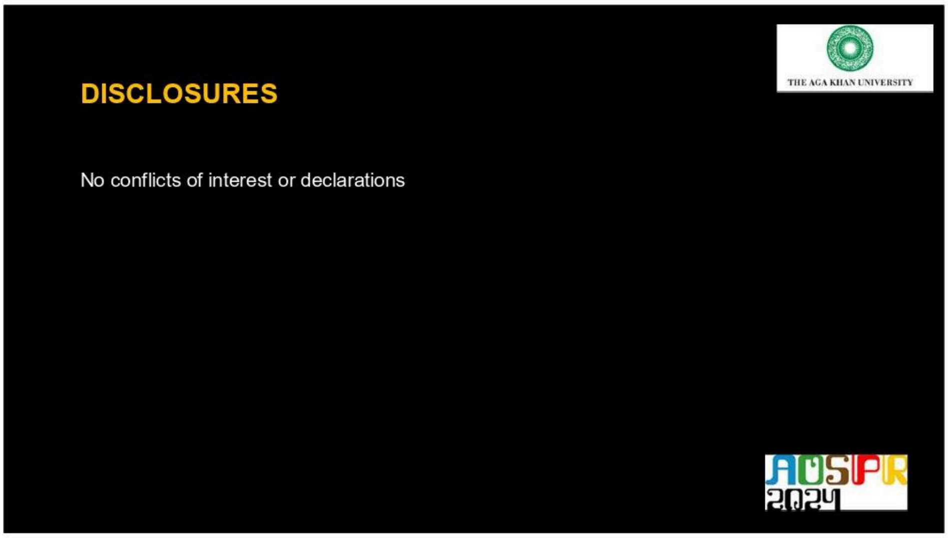

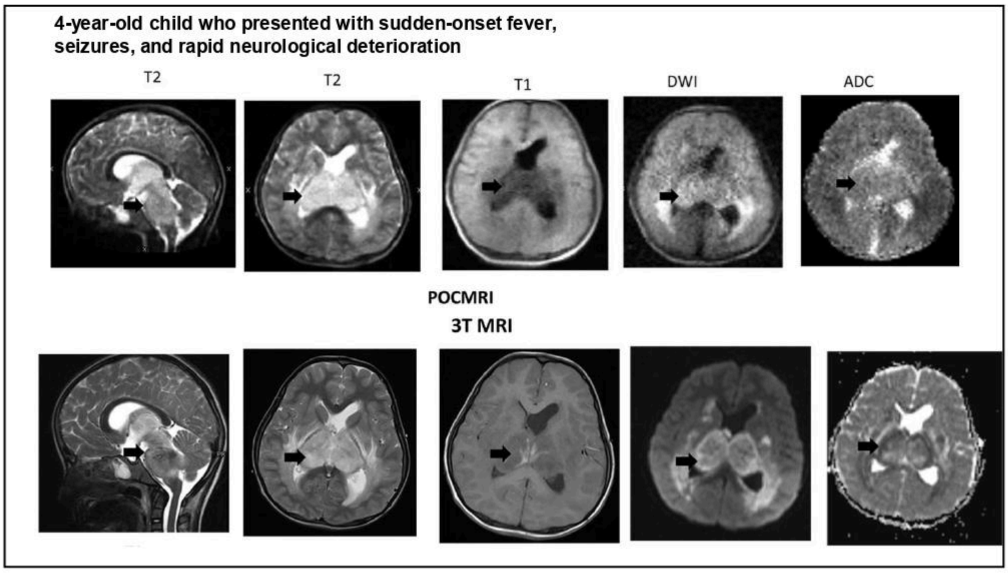
4-year-old child who presented with sudden-onset fever, seizures, and rapid neurological deterioration
T2
T2
T1
DWI
ADC
POCMRI
3T MRI

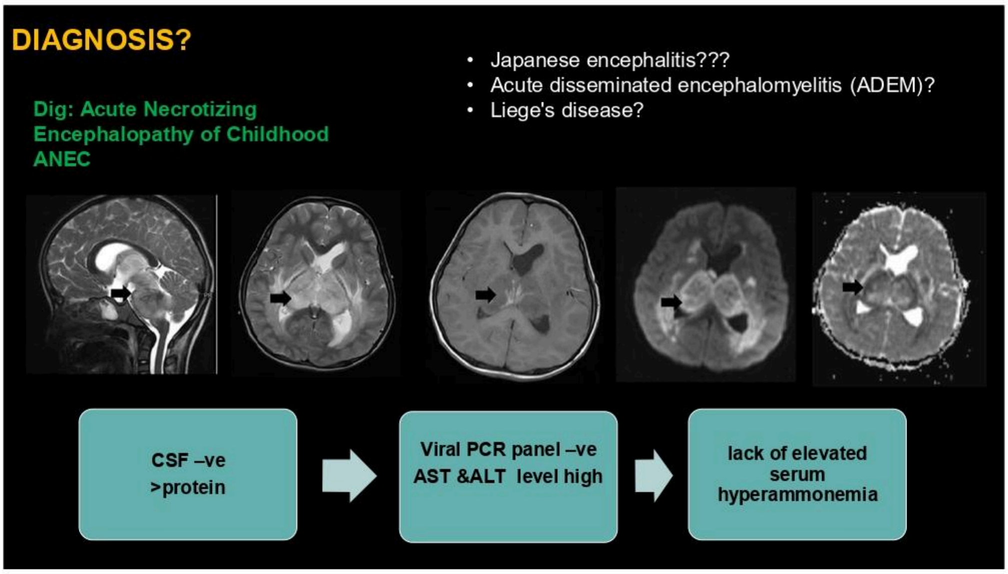
DIAGNOSIS?
Japanese encephalitis???
Acute disseminated encephalomyelitis (ADEM)?
Liege's disease?
Dig: Acute Necrotizing Encephalopathy of Childhood ANEC
CSF –ve >protein
Viral PCR panel –ve AST &ALT level high
lack of elevated serum hyperammonemia

BACKGROUND

- Acute Necrotizing Encephalopathy (ANEC) is a rare, rapidly progressive, and often fatal condition that predominantly affects children, usually following viral infections. It primarily targets the thalami, brainstem, and cerebellum, leading to devastating neurological outcomes.
- It is primarily reported in Asian countries like Japan, Taiwan, Korea, and the subcontinent and has a variable prognosis till date.

CURRENT CHALLENGE

- The current imaging criteria for diagnosing and predicting clinical outcomes in ANEC face significant challenge

Study	Key Features	Limitations
Wong et al. (2006)	Correlation between MRI (thalamic lesions) and clinical outcomes.	Small sample size, no comprehensive score. But the problem with this limitation was
Yamamoto et al. (2015)	Developed a severity score based on lesion location and extent.	Complex to apply, limited validation.
Wu et al. (2015)	Clinicoradiologic approach, highlighted underdiagnosis.	No formal scoring system.

1. **Current MR imaging criteria are too complex and variable.**
2. **Heterogeneity in MR scoring systems.**
3. **Validation on small cohorts.**

A SIMPLIFIED IMAGING APPROACH

- Rationale & Need for Study:
- There is a lack of a standardized tool for predicting ANEC. prognosis
- A **simplified MR-based score** can improve diagnostic accuracy.
- This study leverages the **largest cohort from South Asia**, addressing a crucial gap in current knowledge

THE AGA KHAN UNIVERSITY

AOSPR 2024

THE AGA KHAN UNIVERSITY

A SIMPLIFIED IMAGING APPROACH

- Objective:
- **Develop a simplified , more robust and widely applicable and practical MR scoring system to improve the diagnosis and clinical prognostication of ANEC**

AOSPR 2024

MATERIALS & METHODS

- Retrospective cross-sectional study.
- Study period: 13 years (from 2010 to 2023)
- Inclusion criteria: pediatric patients with ANEC meeting Mizuguchi's criteria.
- Other diseases resembling ANEC were excluded from the study.

Mizuguchi's criteria

- Acute encephalopathy (defined as a sudden decline in consciousness and/or behavioral changes like confusion or irritability)
- The lack of elevated serum hyperammonemia >ALT levels
- The absence of cerebrospinal fluid (CSF) pleocytosis but raised proteins
- Characteristic neuroimaging features displaying bilateral lesions in the thalami

9

Mizuguchi M, Abe J, Mikkaichi K, Noma S, Yoshida K, Yamanaka T, Kamoshita S (1995) Acute necrotizing encephalopathy of childhood: a new syndrome presenting with multifocal, symmetric brain lesions. J Neurol Neurosurg Psychiatry 58:555–561

IMAGING ASSESSMENT

- MR Imaging Examination and Score Development:
- Two pediatric radiologists independently assessed MR imaging variables.
- Developed a simplified MR-based imaging score for acute necrotizing encephalopathy by integrating and modifying approaches from Wong et al. and Ibrahim et al.

- *Wong AM, Simon EM, Zimmerman RA, Wang HS, Toh CH, Ng SH (2006) Acute necrotizing encephalopathy of childhood: Correlation of MR findings and clinical outcome. AJNR Am J Neuroradiol 27:1919-1923.*
- *Ibrahim RSM, Elzayat W, Seif HM, El-Kiki HA, Emad-Eldin S, Shahin M, Kamel SM, Osama R, Zakaryia R, Fatouh M, Hachem RH (2020) Multi-parametric magnetic resonance imaging in acute necrotizing encephalopathy of children: validity and prognostic value. Egypt J Radiol Nucl Med 51:113.*

IMAGING SCORE

THE AGA KHAN UNIVERSITY

AOSPR 2024

1. **Imaging Severity Markers:**
    1. Hemorrhage
    2. Cavitation
    3. Enhancement,
    4. Diffusion Restriction
2. **Involvement of key anatomical regions:**
    - **5.Basal ganglia**
    - **6.Cerebellum**
    - **7.Brainstem**
    - **8.Cerebral white matter**

We initially associated these parameters with clinical outcomes and found that diffusion restriction and cerebellar involvement were the most significant.

- These were given 2 points each, while other parameters were given 1 each.
- The total score, ranging from 0 to 10, was categorized into mild (0-3), moderate (4-7), and severe (8-10).

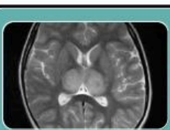

Cavitation

Cavitation was defined as those lesions having sharply defined margins, and CSF intensity with hypointense signal on T1-weighted images and hyperintensity on T2-weighted images with rim enhancement on post contrast images.

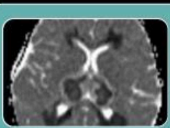

Diffusion restriction

Diffusion restriction was defined by cytotoxic edema appearing bright on diffusion weighted sequences (DWI) and showing dropout on corresponding apparent diffusion coefficient (ADC) maps.

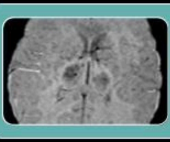

Hemorrhage

The presence of hemorrhage was defined as either petechial or macro-hemorrhages showing signal dropout on SWI sequences.

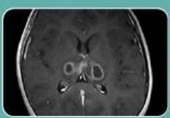

Enhancement

Enhancement was considered positive and defined as either rim enhancement, heterogeneous or intense/avid on T1-post contrast images.

CLINICAL OUTCOME

Clinical outcomes were determined at the time of discharge and on follow-ups by a pediatric neurologist using modified Rankin Scale with scores 0 to 6 ranging from:

- No/mild disability (0 to 2)
- Moderate disability (3 to 4)
- Severe disability (4 to 6)
- Death

13

STATISTICAL ANALYSIS

- SPSS version 20.0.
- Chi-square test, ¥ Fisher Exact Test, € One way ANOVA test was used for statistical analysis and to measure associations.
- P-values less than 0.05 were considered statistically significant.
- **Cohen's Kappa (k)Strength of agreement**

14

RESULTS

CORRELATION WITH CLINICAL PARAMETERS

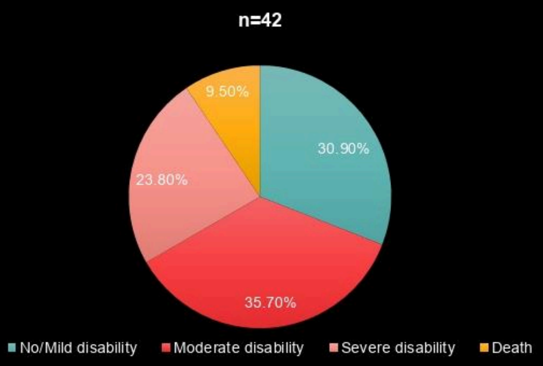

- The clinical outcomes were not significantly associated with
  - length of stay
  - platelet count
  - serum alanine aminotransferase level.
- Presence of shock had a statistically significant association with a worse clinical outcome (p-0.01).
- .

15

RESULTS

Table 2: MR findings and associations with clinical outcome in patients with acute necrotizing encephalopathy of childhood.

	No/Mild Disability (n=13)	Moderate Disability (n=15)	Severe Disability (n=10)	Death (n=4)	P-value
Basal Ganglia	07 (53.8%)	09 (60%)	04 (40%)	03 (75%)	0.6¥
Cerebral White Matter	09 (69.2%)	08 (53.3%)	09 (90%)	03 (75%)	0.2‡
Cerebellum	07 (53.8%)	03 (20%)	03 (30%)	03 (75%)	0.05*¥
Brainstem	10 (77%)	09 (60%)	07 (70%)	04 (100%)	0.5‡
Mamillary Bodies	01 (7.7%)	01 (6.7%)	0 (0.0%)	01 (25%)	0.5‡
External Capsule	03 (23.1%)	05 (33.3%)	04 (40%)	02 (50%)	0.6‡
Hemorrhage	06 (46.2%)	07 (46.7%)	04 (40%)	03 (75%)	0.7¥
Cavitation	05 (38.5%)	05 (33.3%)	05 (50%)	03 (75%)	0.4¥
Enhancement	06 (46.1%)	07 (46.7%)	02 (20%)	03 (75%)	0.2¥
Diffusion Restriction	07 (53.8%)	12 (80%)	09 (90%)	04 (100%)	0.03*‡

* P-value <0.05, ¥ Chi-square test, ‡ Fisher Exact Test

RESULTS

MR Imaging Score Grading	Clinical Outcome			
	Mild disability	Moderate disability	Worst Outcome	P-value
Mild (0 to 3)	8 (44.4)	7 (38.9)	3 (16.7)	0.027* ǂ
Moderate (4 to 7)	2 (10.5)	9 (47.4)	8 (42.1)	
Severe (8 to 10)	0 (0)	1 (20)	4 (80)	
Mean MR Imaging Scores	3 ± 2.21	4.35 ± 2.11	6.13 ± 2.38	0.004* †

* P-value <0.05 was considered as statistically significant

ǂ: Fischer exact test, † One Way ANOVA

RESULTS

Table 3: Inter-rater reliability for different predictors of MRI severity

MR Variables	Percent agreement	Expected agreement (%)	Cohen's Kappa (k)
Thalami	100	-	-
Basal ganglia	90.48	49.89	0.81
Cerebral white matter	78.57	51.36	0.55
Cerebellum	92.86	53.40	0.84
Brainstem	80.95	52.83	0.60
Hemorrhage	95.24	51.02	0.90
Diffusion restriction	90.48	55.1	0.78
Cavitation	78.57	64.97	0.38
Enhancement	76.19	54.54	0.47

Key

Cohen's Kappa (k)	Strength of agreement
0.8 ≥ k	Excellent agreement
0.4 ≤ k < 0.8	Mild to moderate agreement
K<0.4	Poor agreement

Excellent intra-observer reliability with scores of 96% and 93%, respectively

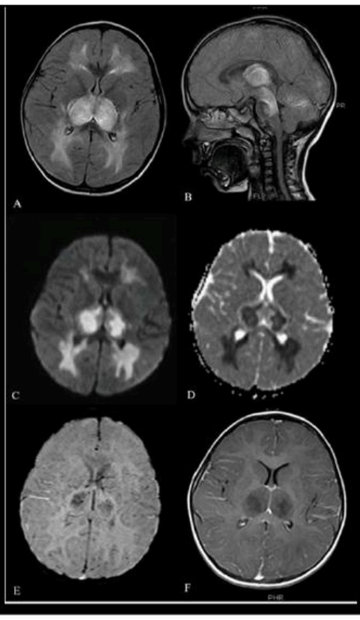

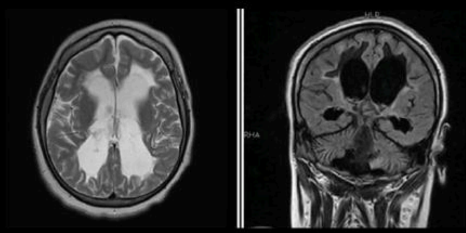

3 yrs old
MR imaging score of 8 with severe long-term disability

DISCUSSION

Key Findings

- A simplified MR-based scoring system was developed, integrating, imaging severity markers, and anatomical locations.
- Diffusion restriction and cerebellar involvement were the most predictive of bad clinical outcomes in ANEC.
- Reliable correlation between imaging findings and clinical prognosis was established, making this scoring system practical in real-world settings.

20

Kim JH, Kim IO, Lim MK, Park MS, Choi CG, Kim HW, Kim JE, Choi SJ, Koh YH, Yang DM, Choo SW, Chung MJ, Yoon HK, Goo HW, Lee M (2004) Acute necrotizing encephalopathy in Korean infants and children: imaging findings and diverse clinical outcome. Korean J Radiol 5:171-177.

THE AGA KHAN UNIVERSITY

DISCUSSION

Comparison to Previous Studies

Brainstem Involvement: Previous studies suggested favorable recovery with brainstem involvement, but in our study, all patients who died had brainstem involvement, though this was not statistically significant.

Hemorrhage and Cavitation: Contrary to Kim et al.'s findings, our study found no significant association between hemorrhage (47.6%) or cavitation (42.9%) and poorer clinical outcomes.

21

Kim JH, Kim IO, Lim MK, Park MS, Choi CG, Kim HW, Kim JE, Choi SJ, Koh YH, Yang DM, Choo SW, Chung MJ, Yoon HK, Goo HW, Lee M (2004) Acute necrotizing encephalopathy in Korean infants and children: imaging findings and diverse clinical outcome. Korean J Radiol 5:171-177.

AOSPR 2024

THE AGA KHAN UNIVERSITY

DISCUSSION

Comparison to Previous Studies

Mortality Rate: Our study showed a mortality rate of 9.5%, significantly lower than the up to 65% reported in previous studies.

Novel Approach: Unlike previous studies, ours uniquely assessed the impact of individual imaging severity and anatomical parameters on clinical outcomes

22

Kim JH, Kim IO, Lim MK, Park MS, Choi CG, Kim HW, Kim JE, Choi SJ, Koh YH, Yang DM, Choo SW, Chung MJ, Yoon HK, Goo HW, Lee M (2004) Acute necrotizing encephalopathy in Korean infants and children: imaging findings and diverse clinical outcome. Korean J Radiol 5:171-177.

AOSPR 2024

LIMITATIONS

- Single center study, relatively small sample size due to disease rarity
- We had no resources to carry out the RANBP2 target mutation and therefore could not determine a genetic analysis.
- Timing of MR brain scans was not considered, and some features may have been underrepresented since radiological features of ANEC (such as hemorrhage and cavitation) can evolve over time.
- Our follow-ups were limited because not all patients could be clinically examined, and we had few patients with follow-up imaging.

CONCLUSION & FUTURE DIRECTIONS

- ANEC's **complexity** demands a robust MR-based severity scoring system for better diagnosis and outcomes prediction
- Diffusion restriction and cerebellar involvement are crucial for prognostication
- **Future direction**: Standardized imaging protocols and genetic testing will help refine and validate the current scoring system for better patient outcomes

Wong AM, Simon EM, Zimmerman RA, Wang HS, Toh CH, Ng SH (2006) Acute necrotizing encephalopathy of childhood: Correlation of MR findings and clinical outcome. AJNR Am J Neuroradiol 27:1919-1923.


The Aga Khan University
THE AGA KHAN UNIVERSITY
Thank You
Questions?
Email: kiran.hilal@aku.edu
@KiranHilal1
linkedin.com/in/dr-kiran-hilal
Kiran Hilal
AOSPR 2024

A Pictorial Review of Paediatric Head and Neck Masses

Nadia Fareeda Muhammad Gowdh[1,2,3], Faizah Mohd Zaki[2], Rohazly Ismail[3]

[1] *Biomedical Imaging Department, Faculty of Medicine, Universiti Malaya, Malaysia*
[2] *Radiology Department, Children Specialist Hospital, Universiti Kebangsaan Malaysia, Malaysia*
[3] *Radiology Department, Hospital Tunku Azizah, Kuala Lumpur, Malaysia*

22nd Annual Scientific Meeting of Asian and Oceanic Society for Pediatric Radiology (AOSPR) 2024

1

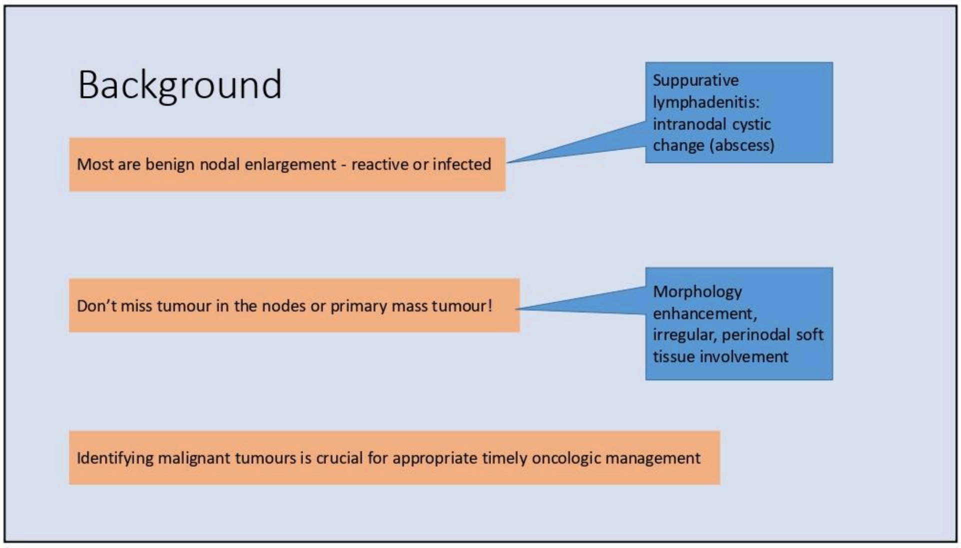

2

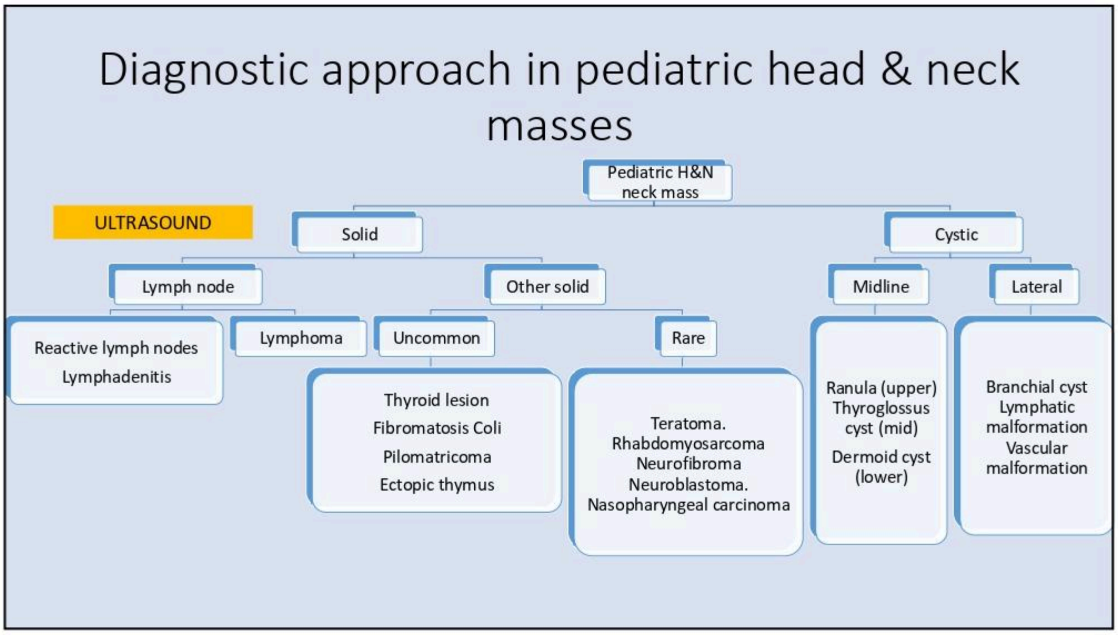
Diagnostic approach in pediatric head & neck masses
ULTRASOUND
Pediatric H&N neck mass
Solid
Cystic
Lymph node
Other solid
Midline
Lateral
Reactive lymph nodes
Lymphadenitis
Lymphoma
Uncommon
Rare
Thyroid lesion
Fibromatosis Coli
Pilomatricoma
Ectopic thymus
Teratoma.
Rhabdomyosarcoma
Neurofibroma
Neuroblastoma.
Nasopharyngeal carcinoma
Ranula (upper)
Thyroglossus cyst (mid)
Dermoid cyst (lower)
Branchial cyst
Lymphatic malformation
Vascular malformation

3

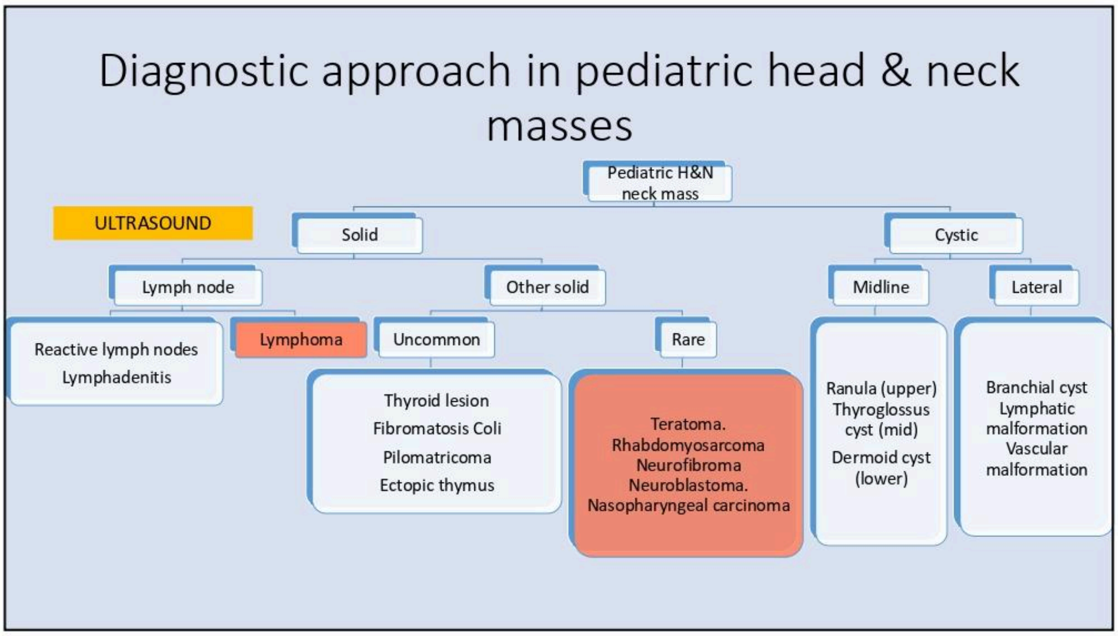
Diagnostic approach in pediatric head & neck masses
ULTRASOUND
Pediatric H&N neck mass
Solid
Cystic
Lymph node
Other solid
Midline
Lateral
Reactive lymph nodes
Lymphadenitis
Lymphoma
Uncommon
Rare
Thyroid lesion
Fibromatosis Coli
Pilomatricoma
Ectopic thymus
Teratoma.
Rhabdomyosarcoma
Neurofibroma
Neuroblastoma.
Nasopharyngeal carcinoma
Ranula (upper)
Thyroglossus cyst (mid)
Dermoid cyst (lower)
Branchial cyst
Lymphatic malformation
Vascular malformation

4

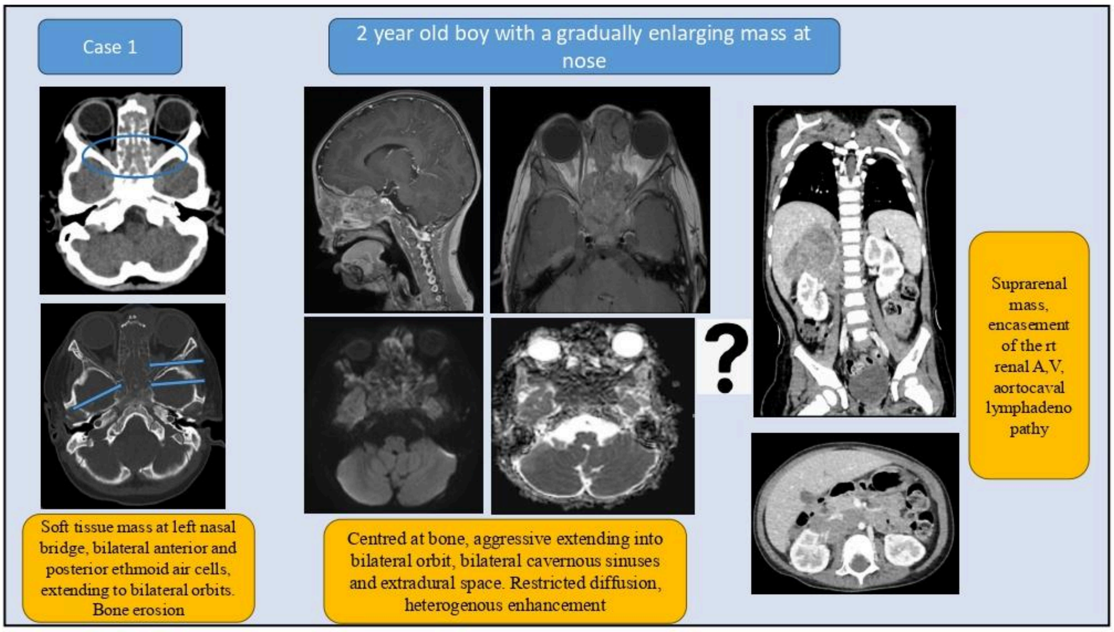
Case 1
2 year old boy with a gradually enlarging mass at nose
?
Suprarenal mass, encasement of the rt renal A,V, aortocaval lymphadeno pathy
Soft tissue mass at left nasal bridge, bilateral anterior and posterior ethmoid air cells, extending to bilateral orbits. Bone erosion
Centred at bone, aggressive extending into bilateral orbit, bilateral cavernous sinuses and extradural space. Restricted diffusion, heterogenous enhancement

5

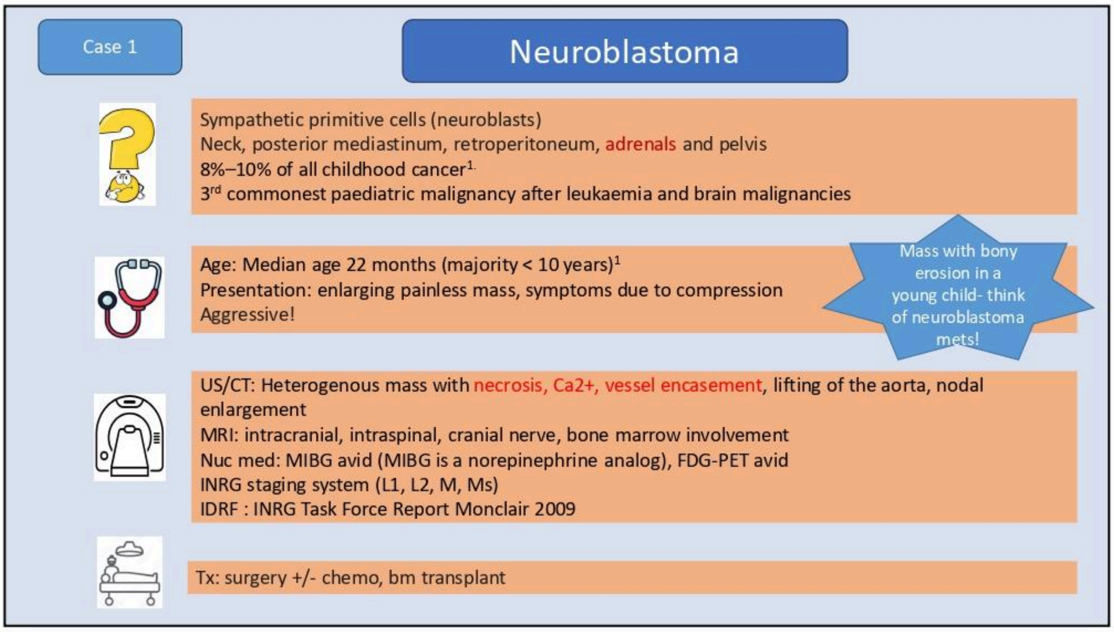
Case 1
Neuroblastoma
Sympathetic primitive cells (neuroblasts)
Neck, posterior mediastinum, retroperitoneum, adrenals and pelvis
8%–10% of all childhood cancer[1.]
3rd commonest paediatric malignancy after leukaemia and brain malignancies
Age: Median age 22 months (majority < 10 years)[1]
Presentation: enlarging painless mass, symptoms due to compression
Aggressive!
Mass with bony erosion in a young child- think of neuroblastoma mets!
US/CT: Heterogenous mass with necrosis, Ca2+, vessel encasement, lifting of the aorta, nodal enlargement
MRI: intracranial, intraspinal, cranial nerve, bone marrow involvement
Nuc med: MIBG avid (MIBG is a norepinephrine analog), FDG-PET avid
INRG staging system (L1, L2, M, Ms)
IDRF : INRG Task Force Report Monclair 2009
Tx: surgery +/- chemo, bm transplant

6

Case 2

5-month old girl with a 3-month history of progressively enlarging painless left cervical mass. Not resolved with antibiotic therapy. US done TRO reactive lymphadenopathy

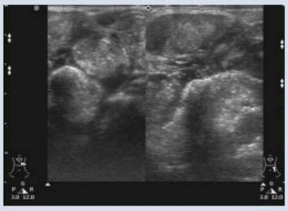

Multiple, matted enlarged left cervical lymphadenopathy. Hyperechoiec areas suggestive of calcification

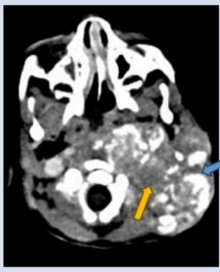

Multiple enhancing nodular lesions in the left carotid space and posterior triangle, necrosis, calcification

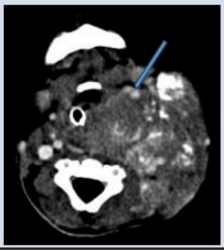

Lt carotid vessels displased anteriorly

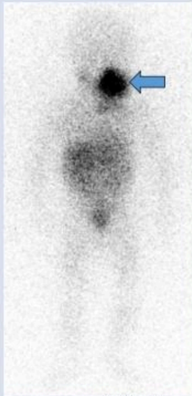

MIBG: high uptake at the left cervical mass only. No increased uptake elsewhere

7

Case 2

Primary cervical neuroblastoma

Incidence of primary cervical neuroblastoma : < 5% of all neuroblastomas[2]
Arises from the superior cervical ganglion behind the ICA
Posterior to the vascular sheet, displacing the carotid artery, IJV anteriorly

Age: More common in infants[2]
Presentation: Enlarging painless lateral neck mass, symptoms due to compression
Ds pattern: Aggressive behavior - can invade the cranial nerves

Ultrasound usually primary imaging tool
CT/MRI for further characterization (MRI superior)

Tx: surgery
Favourable outcome of infant neuroblastoma.
The overall five-year survival rate of cervical neuroblastoma is around 90% [2]

8

Case 3

5 year old boy with left neck swelling x 2weeks. External CT noted to have left neck mass.

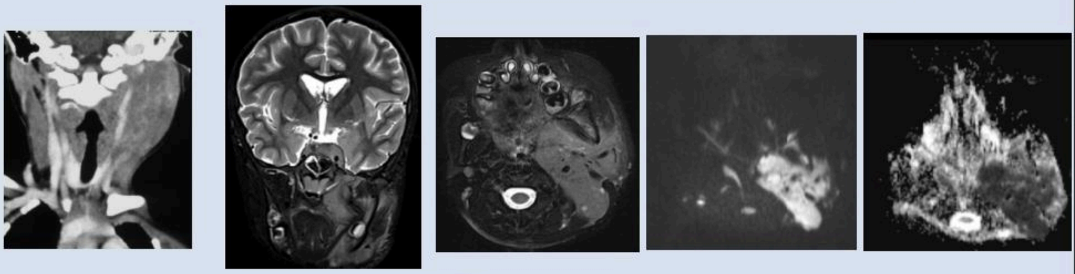

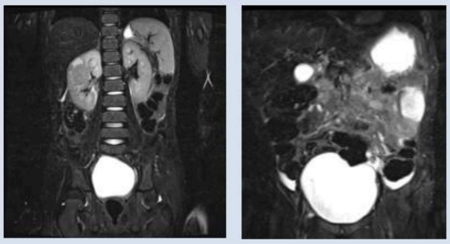

Matted enlarged left cervical lymphadenopathy, palatine tonsil, adenoid involvement with restricted diffusion, prominent right cervical node, bilateral cavernous sinus and rt renal, abdominal nodal involvement

9

Case 3

Burkitt lymphoma (Non-Hodgkin Lymphoma)

Aggressive B-cell lymphoma predominantly affecting children
Most common (40%) type of non-Hodgkin lymphoma in childhood

Age: Median age is 8 years[4]
Male predominance (M:F = 4:1)
Presentation: enlarging mass
Beware of airway compromise!

Ultrasound, CT/MRI
Solid lobulated mass, predilection for the Waldeyer's ring, restricted diffusion (highly cellular), T2W isointense (highly cellular), homogenous enhancement
(absence of necrosis and bone destruction supports Burkitt's lymphoma)[5]

Curable, highly sensitive to chemotherapy

10

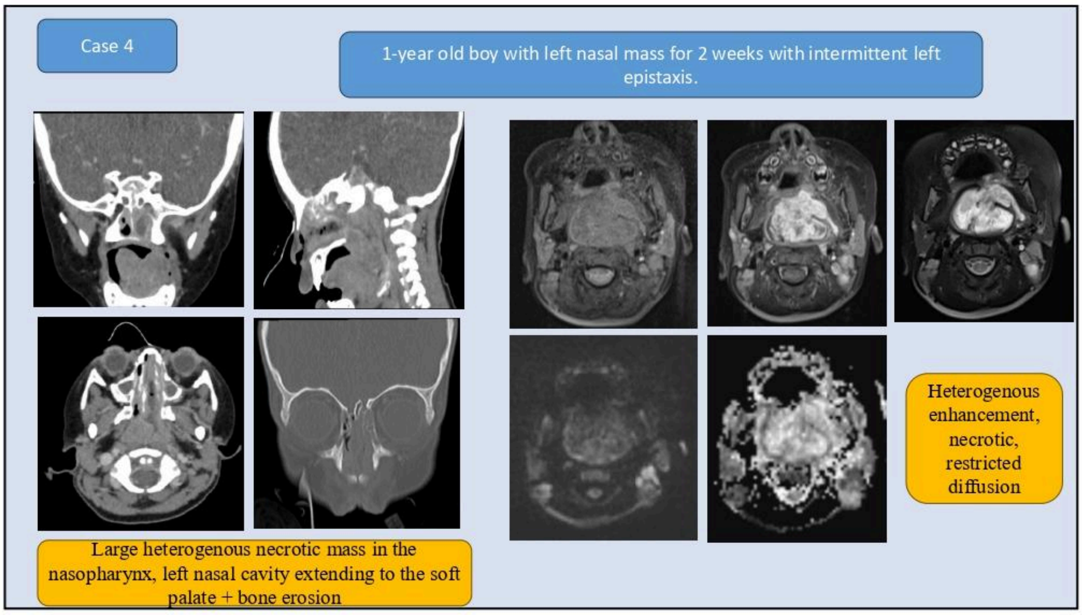
Case 4
1-year old boy with left nasal mass for 2 weeks with intermittent left epistaxis.
Heterogenous enhancement, necrotic, restricted diffusion
Large heterogenous necrotic mass in the nasopharynx, left nasal cavity extending to the soft palate + bone erosion

11

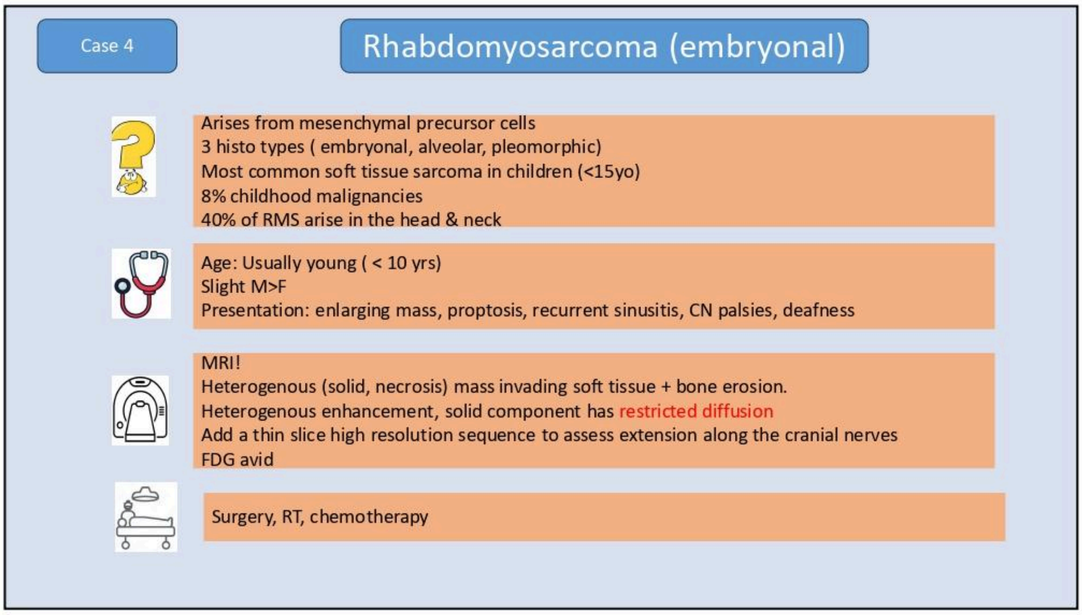
Case 4
Rhabdomyosarcoma (embryonal)
Arises from mesenchymal precursor cells
3 histo types (embryonal, alveolar, pleomorphic)
Most common soft tissue sarcoma in children (<15yo)
8% childhood malignancies
40% of RMS arise in the head & neck
Age: Usually young (< 10 yrs)
Slight M>F
Presentation: enlarging mass, proptosis, recurrent sinusitis, CN palsies, deafness
MRI!
Heterogenous (solid, necrosis) mass invading soft tissue + bone erosion.
Heterogenous enhancement, solid component has restricted diffusion
Add a thin slice high resolution sequence to assess extension along the cranial nerves
FDG avid
Surgery, RT, chemotherapy

12

Case 5

10 year old boy with left neck swelling since 4 months associated with diplopia (left lateral rectus palsy since 3 weeks).
Nasoendoscopy: lobulated mass occupying the nasopharynx

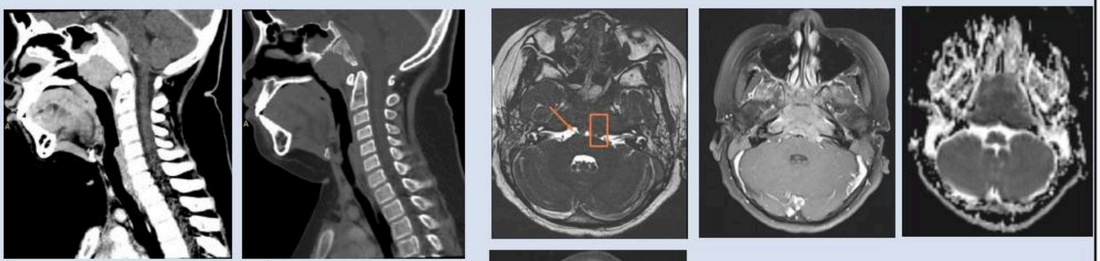

Large enhancing mass in the nasopharynx with intracranial extradural extension + erosion of the sphenoid and clivus

Enhancing, restricted nasopharyngeal mass with extradural mass.
Preponine cisternal component obscuring the left CNVI

13

Case 5

Nasopharyngeal carcinoma

Childhood NPC is rare
Associated with EBV infection
Most childhood NPC histology: undifferentiated carcinoma (WHO subtype III)

Age: Median 13 yo
Slight M>F
Presentation: upper cervical mass, CN involvement, regional nodal involvement, conductive deafness mass, proptosis, recurrent sinusitis, CN palsies, deafness

CT & MRI
CT- better for bone erosion. Homogenously enhancing soft tissue mass + skull base erosion.
Necrotic nodes less common compared to adults
MRI – Slightly hyperintense to muscle on T1W, T2W with homogenous enhancement
CT thorax for staging

High dose RT, chemotherapy

14

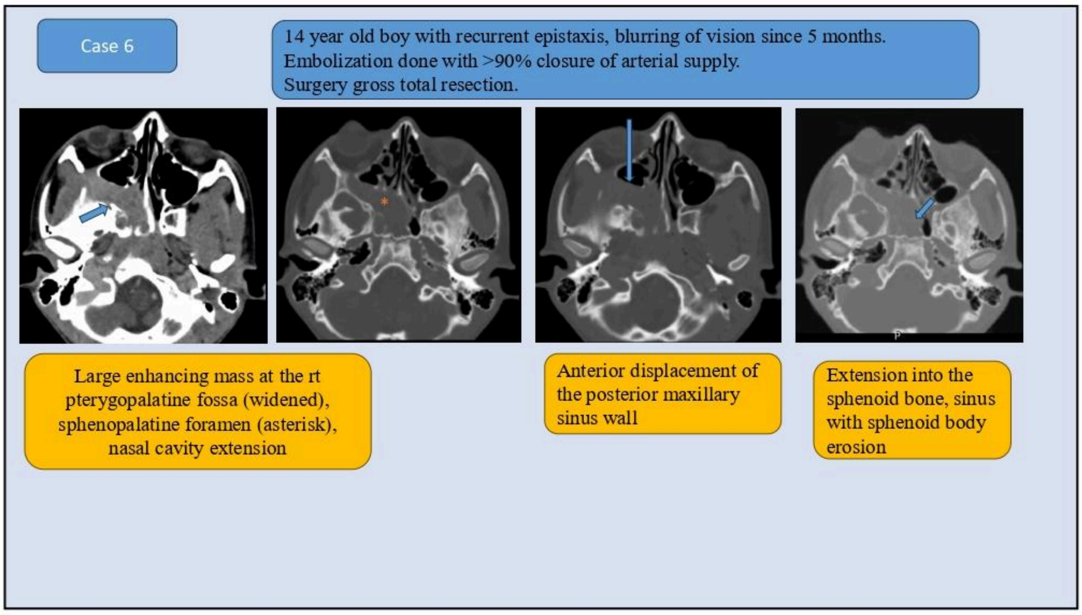
Case 6
14 year old boy with recurrent epistaxis, blurring of vision since 5 months.
Embolization done with >90% closure of arterial supply.
Surgery gross total resection.
Large enhancing mass at the rt pterygopalatine fossa (widened), sphenopalatine foramen (asterisk), nasal cavity extension
Anterior displacement of the posterior maxillary sinus wall
Extension into the sphenoid bone, sinus with sphenoid body erosion

15

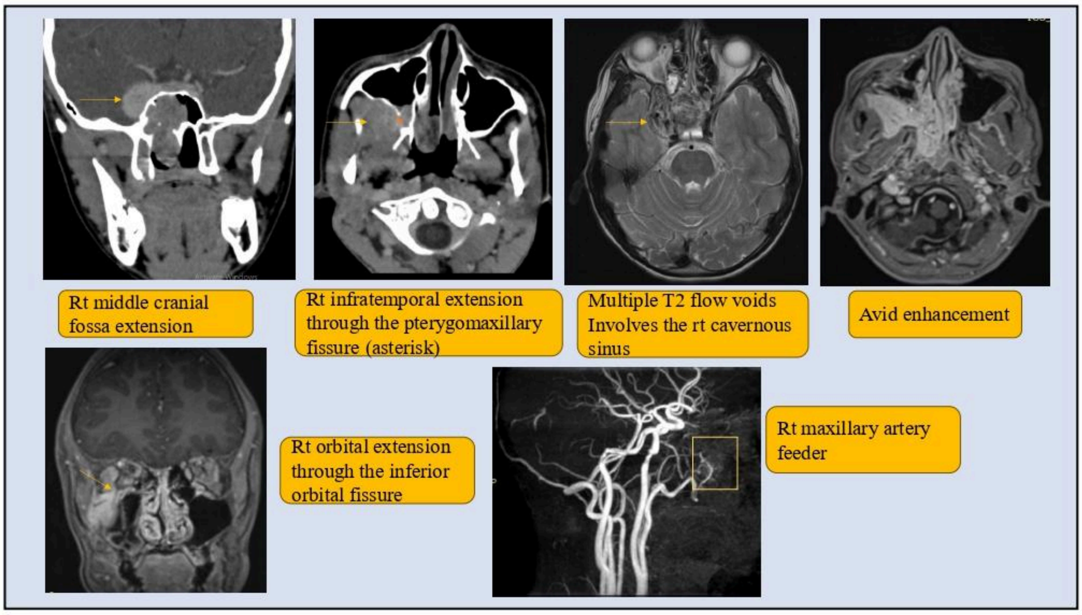
Rt middle cranial fossa extension
Rt infratemporal extension through the pterygomaxillary fissure (asterisk)
Multiple T2 flow voids Involves the rt cavernous sinus
Avid enhancement
Rt orbital extension through the inferior orbital fissure
Rt maxillary artery feeder

16

Case 6

Juvenile angiofibroma

Highly vascular tumour
Posterior nasal cavity and nasopharynx
Locally aggressive
Tends to recur
Arises from the pterygopalatine fossa

Almost all are adolescent males
Presentation: nasal obstruction, epistaxis

CT + MRI
CT: useful for assessment of bone erosion and extension into sphenoid
Nasal cavity mass + pterygopalatine fossa + bone erosion behind the sphenopalatine foramen = JA
MRI: flow voids, enhancement ++ (very vascular)

Endoscopic surgical resection +/- RT, pre-op embolization

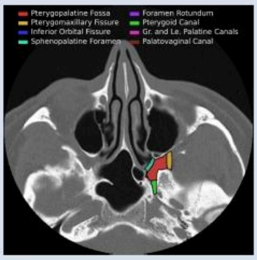

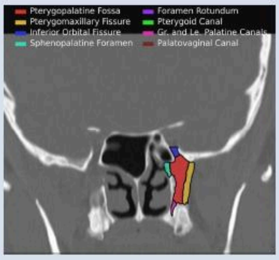

Case courtesy of Reuben Schmidt, Radiopaedia.org, rID: 177576

17

Key points

- Look for restricted diffusion -it can guide diagnosis
- Look at the extent of the tumour- it can insinuate (thin slice volumetric images are useful)
- Consider primary tumour or metastasis (in a young children with a lesion centred at bone always screen the abdomen for neuroblastoma)
- If multifocal tumours, think of an underlying genetic cancer predisposition syndrome
- Also consider differentials such as abscess (think of TB in our population)

18

Conclusion

Imaging plays a key role in diagnosis and follow-up of pediatric head and neck masses

Recognizing the imaging characteristics will improve diagnostic confidence and facilitate prompt diagnosis and management of malignant tumours

19

References

1. Lonergan GJ, Schwab CM, Suarez ES, Carlson CL. From the archives of the AFIP: neuroblastoma, ganglioneuroblastoma, and ganglioneuroma: radiologic-pathologic correlation. Radiographics. 2002 Jul;22(4):911-34.
2. Csanády M, Vass G, Bartyik K, Majoros V, Rovó L. Multidisciplinary management of cervical neuroblastoma in infants. International journal of pediatric otorhinolaryngology. 2014 Dec 1;78(12):2103-6.
3. Haddad M, Triglia JM, Helardot P, Couanet D, Gauthier F, Neuenschwander S, Bourlière B, Bergeron C, Munzer C, Rubie H, Guys JM. Localized cervical neuroblastoma: prevention of surgical complications. International journal of pediatric otorhinolaryngology. 2003 Dec 1;67(12):1361-7.
4. Biko DM, Anupindi SA, Hernandez A, Kersun L, Bellah R. Childhood Burkitt lymphoma: abdominal and pelvic imaging findings. American Journal of Roentgenology. 2009 May;192(5):1304-15.
5. Derinkuyu BE, Boyunağa Ö, Öztunalı Ç, Tekkeşin F, Damar Ç, Alımlı AG, Okur A. Imaging features of Burkitt lymphoma in pediatric patients. Diagnostic and Interventional Radiology. 2016 Jan;22(1):95
6. Lloyd C, McHugh K. The role of radiology in head and neck tumours in children. Cancer Imaging. 2010;10(1):49.
7. The Radiology Assistant. https://radiologyassistant.nl/head-neck/neck-masses/neck-masses-in-children#introduction-diagnostic-approach

20

21

Preventing Thermal Injury in Percutaneous Image-guided Ablation in Children - How Useful are Thermo-protective Strategies? A 5-year Retrospective Review

Way Loon Jonathan CHEN[1], Kin Fen Kevin FUNG[1], Hing Yan Danny CHO[2], Elaine Kan[1]

[1] *Department of Radiology, Hong Kong Children's Hospital, Hong Kong*
[2] *Department of Diagnostic and Interventional Radiology, Kwong Wah Hospital, Hong Kong SAR*

22nd Annual Scientific Meeting of Asian and Oceanic Society for Pediatric Radiology

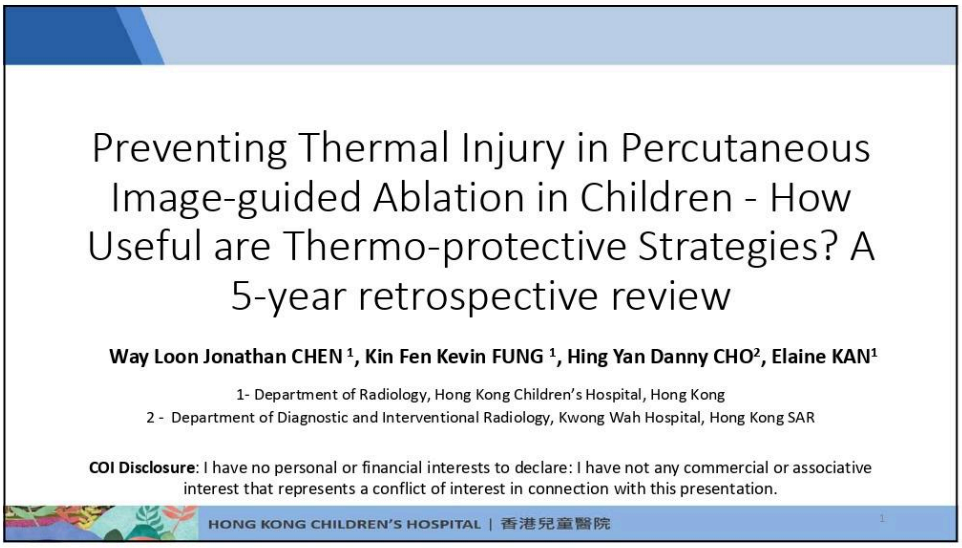

1

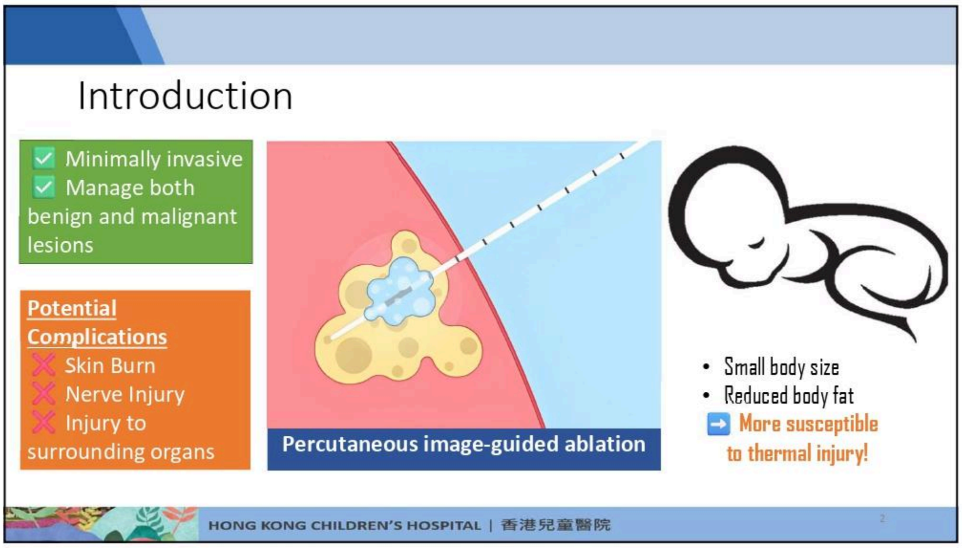

2

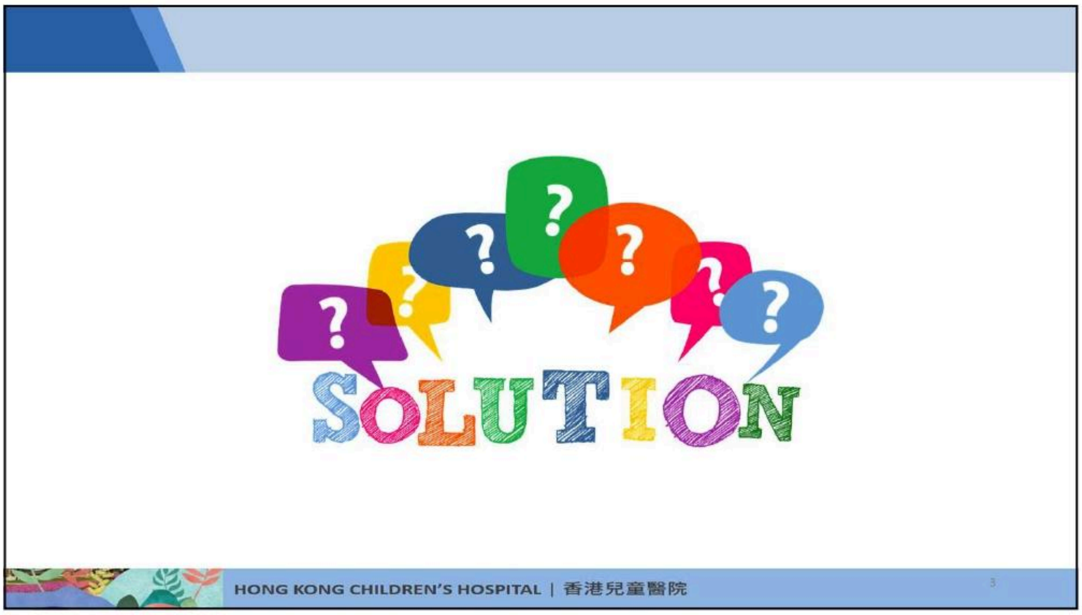
SOLUTION
HONG KONG CHILDREN'S HOSPITAL | 香港兒童醫院

3

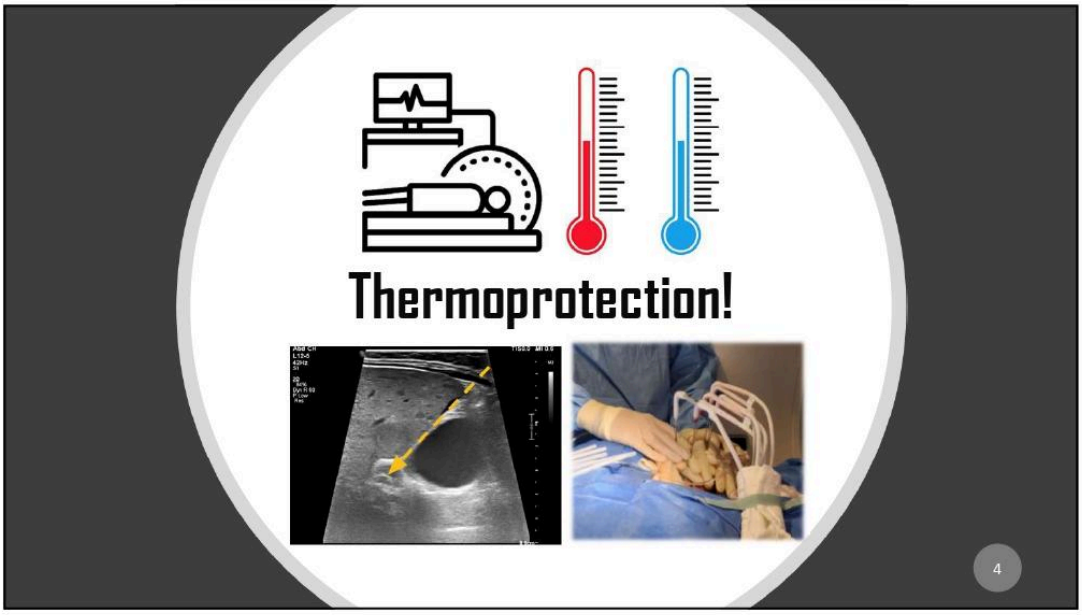
Thermoprotection!
4

4

Passive Thermoprotection: Neurophysiological Monitoring

- Under supervision of **on-site neurophysiologist**.
- **Continuous monitoring throughout procedure**.
- **Termination of freezing** (for cryoablation) following **significant SEP** and/or **MEP amplitude drop**.

HONG KONG CHILDREN'S HOSPITAL | 香港兒童醫院

5

Passive Thermoprotection: Temperature Monitoring

- **Intermittent screening** with **infra-red temperature gun**.
- **Real-time image monitoring** of **iceball / ablation zone**.

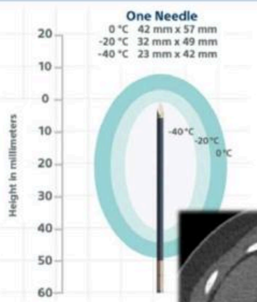

HONG KONG CHILDREN'S HOSPITAL | 香港兒童醫院

6

Active Thermoprotection

- **Hydrodissection** of **skin** & **fascial space**
- Creation of **artificial effusions**
- **Direct blunt needle displacement** of **intra-abdominal organs**

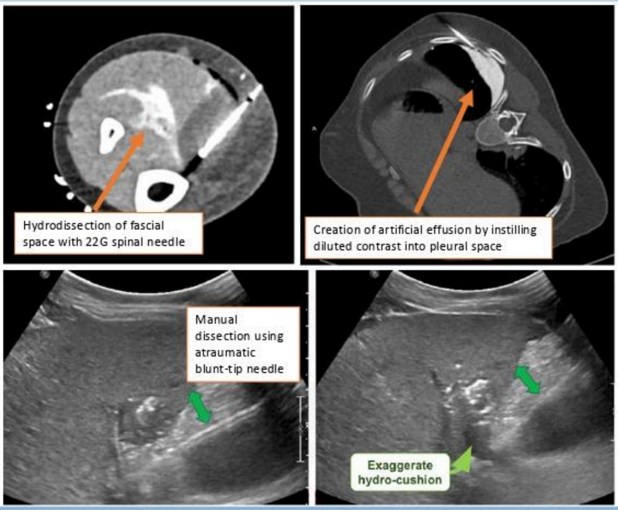

Active Thermoprotection (cont.)

- **Warm gloves** applied to skin surface.

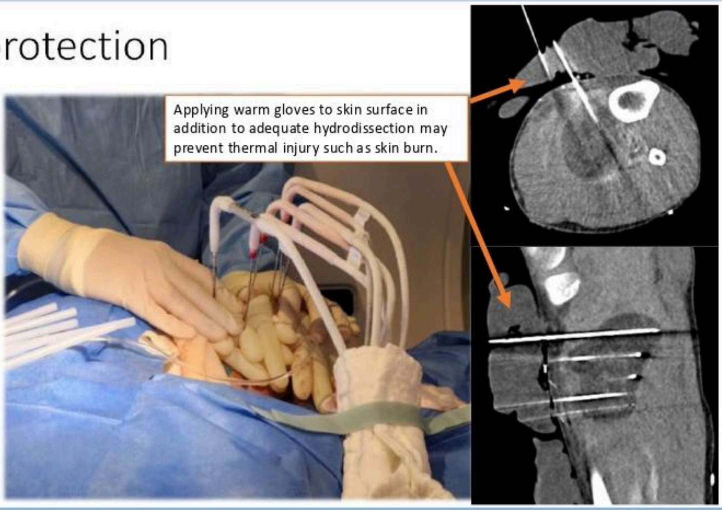

Purpose

To evaluate the utility of **thermo-protective measures** in **preventing thermal injury during ablation** in the **paediatric population.**

HONG KONG CHILDREN'S HOSPITAL | 香港兒童醫院

9

9

Materials and Methods

- **Retrospective** review.
- All patients undergoing image-guided percutaneous ablation of soft tissue lesions at our tertiary children's hospital from **June 2019** to **June 2024**.
- All patients underwent cross-sectional imaging with CT or MRI prior to, and after the procedure.

HONG KONG CHILDREN'S HOSPITAL | 香港兒童醫院

10

10

Materials and Methods

Parameters assessed:

- **Indications for image-guided percutaneous ablation**: included both neoplastic and non-neoplastic conditions for which ablation was performed either as a definitive or palliative therapy.
- **Modality of percutaneous ablation**.
- **Lesion characteristics**: ie location, size, volume, proximity to adjacent structures / organs.
- **Thermoprotective strategies deployed**: ie active vs passive.
- **Complications**.
- **Clinical Outcomes.**

HONG KONG CHILDREN'S HOSPITAL | 香港兒童醫院 11

11

Results

Lesion number	Location	Pathology	Volume (cm^3)	Type of Ablation	Complications (Y/N)
1	Posterior Rib	Osteosarcoma	4.3	Cryoablation	N
2	Anterior Rib	Osteosarcoma	5.6	Cryoablation	N
3	Left Calf	Desmoid tumour	270.6	Microwave Ablation	N
4	Kidney	Indeterminate renal lesion	8.5	Cryoablation	N
5	Liver	Hepatic Adenoma	14.7	Microwave Ablation	N
6	Liver	Hepatic Adenoma	8.0	Microwave Ablation	N
7	Liver	Hepatic Adenoma	8.0	Microwave Ablation	N
8	Liver	Hepatic Adenoma	8.0	Microwave Ablation	N
9	Liver	Hepatic Adenoma	4.0	Microwave Ablation	N
10	Liver	Hepatic Adenoma	6.2	Microwave Ablation	N
11	Liver	HCC	8.6	Microwave Ablation	N
12	Liver	HCC	11.3	Microwave Ablation	N
13	Supraclavicular fossa	Desmoid tumour	215.0	Cryoablation	Y
14	Left Calf	Desmoid Tumour	484.7	Cryoablation	Y

HONG KONG CHILDREN'S HOSPITAL | 香港兒童醫院 12

12

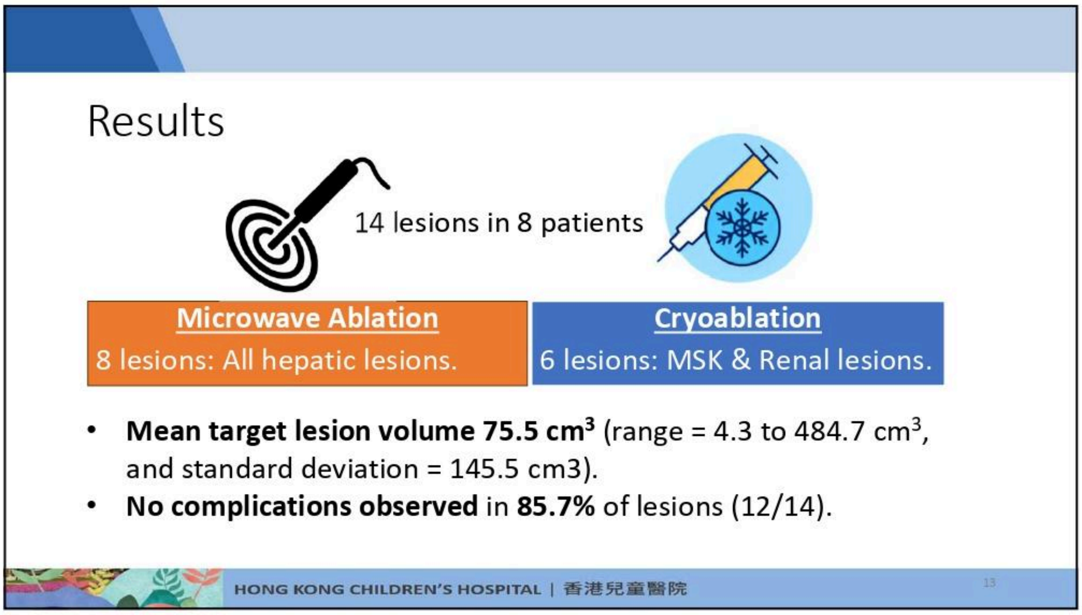
Results
14 lesions in 8 patients
Microwave Ablation
8 lesions: All hepatic lesions.
Cryoablation
6 lesions: MSK & Renal lesions.
• Mean target lesion volume 75.5 cm³ (range = 4.3 to 484.7 cm³, and standard deviation = 145.5 cm3).
• No complications observed in 85.7% of lesions (12/14).
HONG KONG CHILDREN'S HOSPITAL | 香港兒童醫院
13

13

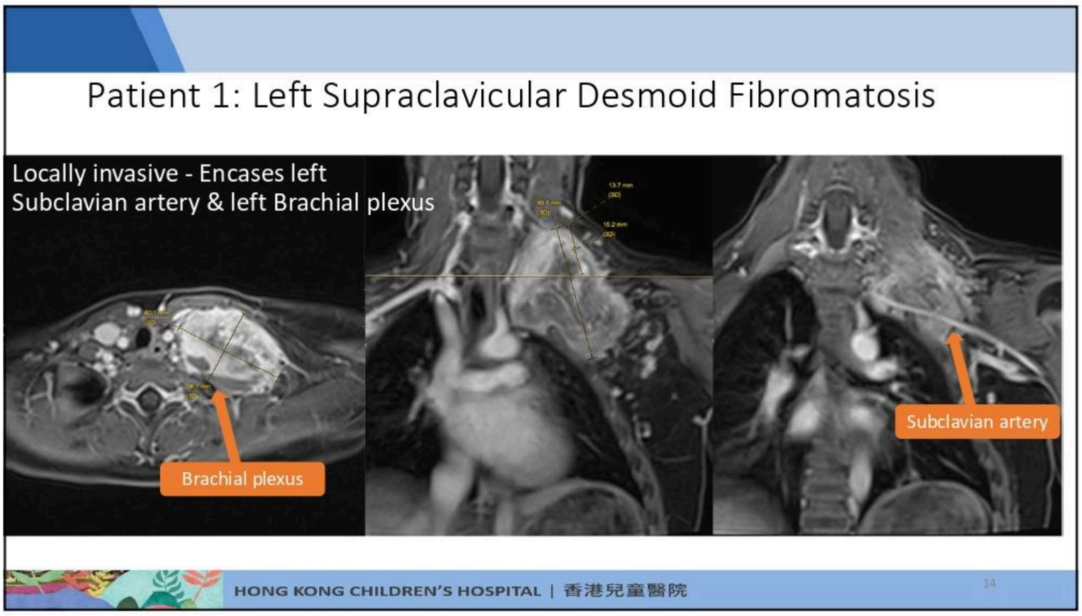
Patient 1: Left Supraclavicular Desmoid Fibromatosis
Locally invasive - Encases left
Subclavian artery & left Brachial plexus
Brachial plexus
Subclavian artery
HONG KONG CHILDREN'S HOSPITAL | 香港兒童醫院
14

14

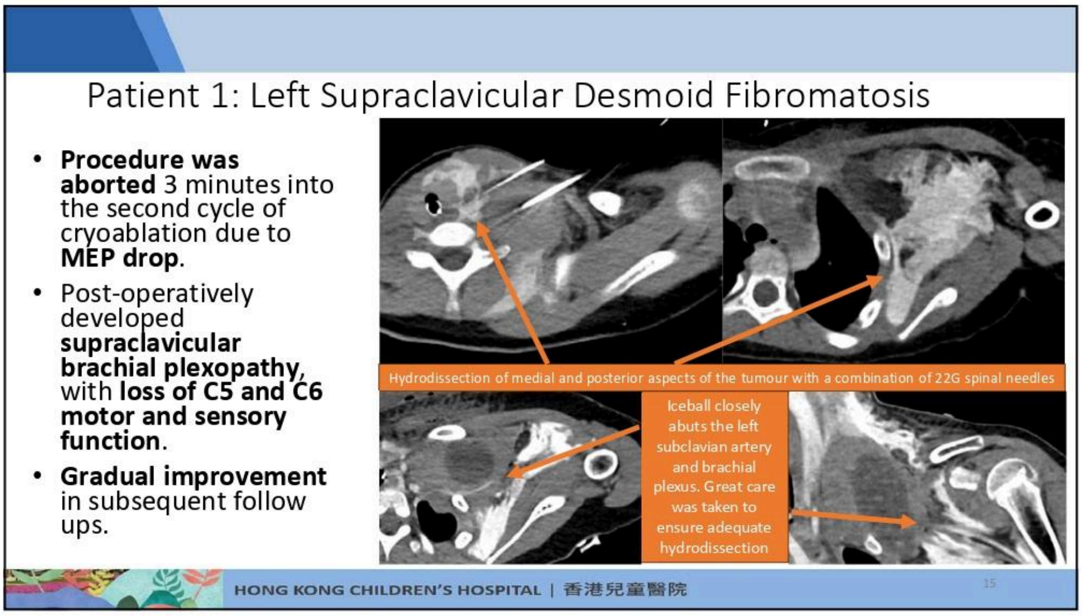
Patient 1: Left Supraclavicular Desmoid Fibromatosis
• Procedure was aborted 3 minutes into the second cycle of cryoablation due to MEP drop.
• Post-operatively developed supraclavicular brachial plexopathy, with loss of C5 and C6 motor and sensory function.
• Gradual improvement in subsequent follow ups.
Hydrodissection of medial and posterior aspects of the tumour with a combination of 22G spinal needles
Iceball closely abuts the left subclavian artery and brachial plexus. Great care was taken to ensure adequate hydrodissection
HONG KONG CHILDREN'S HOSPITAL | 香港兒童醫院
15

15

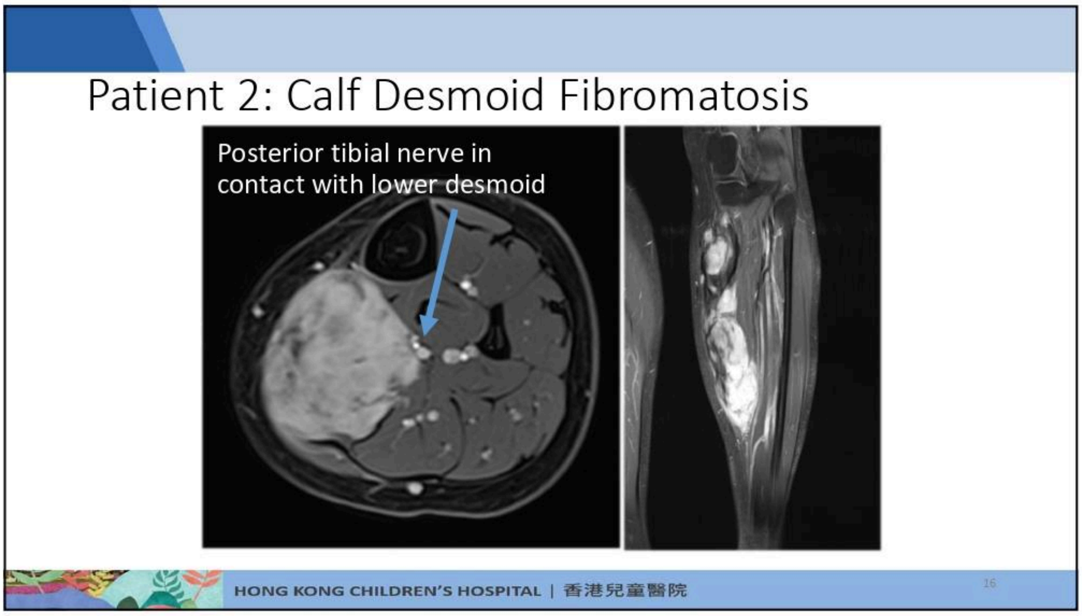
Patient 2: Calf Desmoid Fibromatosis
Posterior tibial nerve in contact with lower desmoid
HONG KONG CHILDREN'S HOSPITAL | 香港兒童醫院
16

16

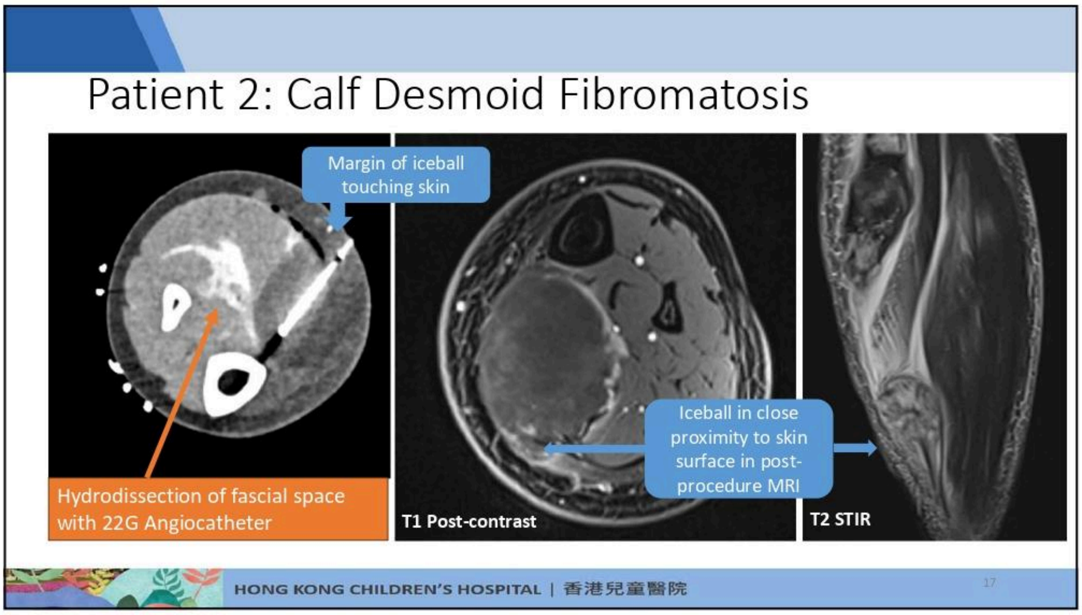
Patient 2: Calf Desmoid Fibromatosis
Margin of iceball touching skin
Iceball in close proximity to skin surface in post-procedure MRI
Hydrodissection of fascial space with 22G Angiocatheter
T1 Post-contrast
T2 STIR
HONG KONG CHILDREN'S HOSPITAL | 香港兒童醫院
17

17


Patient 2: Calf Desmoid Fibromatosis
• 2nd degree burn, complicated with Methicillin-sensitive Staphylococcus aureus wound infection.
• Attributed to inadequate coverage of skin with warm gloves and suboptimal visualisation of iceball in subcutaneous fat.
1 hour
3 hours
1 week
Fully healed, ~1 month post procedure
HONG KONG CHILDREN'S HOSPITAL | 香港兒童醫院
18

18

Discussion

- **Thermoprotective strategies** were **generally effective** in **preventing thermal injury related complications**.
- **Complications** were observed in lesions with **larger tumour volume** and those which **tumour debulking** was the treatment goal (vs total removal).

Limitations

- **Small cohort**.
- **Heterogeneous spectrum of lesions**.
- **Confounding factors**.

Key Takeaways

- **Careful pre-operative planning** for **optimal ablation zone size**.
- **Utilization of the various thermoprotection techniques** on a case-by-case basis.
- **Visualisation of ablation zone**: improves predictability of tumour coverage and prevents non-target ablation.

Coverage of skin with warm gloves

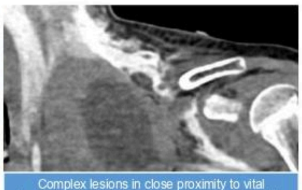

Complex lesions in close proximity to vital structures can pose challenges for hydrodissection

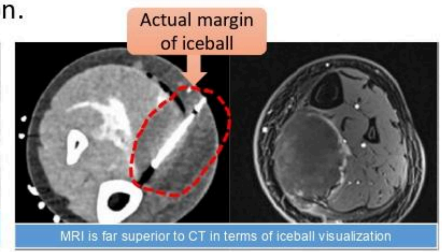

MRI is far superior to CT in terms of iceball visualization

References

1. Filippiadis DK, Binkert C, Pellerin O, Hoffmann RT, Krajina A, Pereira PL. Cirse Quality Assurance Document and Standards for Classification of Complications: The Cirse Classification System. CardioVascular and Interventional Radiology. 2017 Jun 5;40(8):1141–6.
2. Anil Nicholas Kurup, Morris JM, Boon AJ, Strommen JA, Schmit GD, Atwell TD, et al. Motor Evoked Potential Monitoring during Cryoablation of Musculoskeletal Tumors. Journal of Vascular and Interventional Radiology. 2014 Nov 1;25(11):1657–64.
3. Kumar Kempegowda Shashi, Shahin MM, Johnston P, Shaikh R. Cryoablation for Bone and Soft Tissue Lesions in Pediatric Patients: Complications and Preventive Measures. CardioVascular and Interventional Radiology. 2023 Aug 14;46(9):1249–56.
4. Alan Alper Sag, Husain AM. Thermal Protection Strategies and Neuromonitoring during Ablation. Seminars in Interventional Radiology. 2022 Apr 1;39(02):157–61.

HONG KONG CHILDREN'S HOSPITAL | 香港兒童醫院 21

21

22

Use of Multiparametric MRI in Evaluating Posterior Fossa Tumors in Pediatric Filipino Cohort

Kim Ivan R. Mendoza, Cyruz Jan B. David, Dan Philippe C. Nicer, Rovi Nino D. Samedra

Department of Radiology, University of the Philippines - Philippine General Hospital, Philippines

22nd Annual Scientific Meeting of Asian and Oceanic Society for Pediatric Radiology (AOSPR) 2024

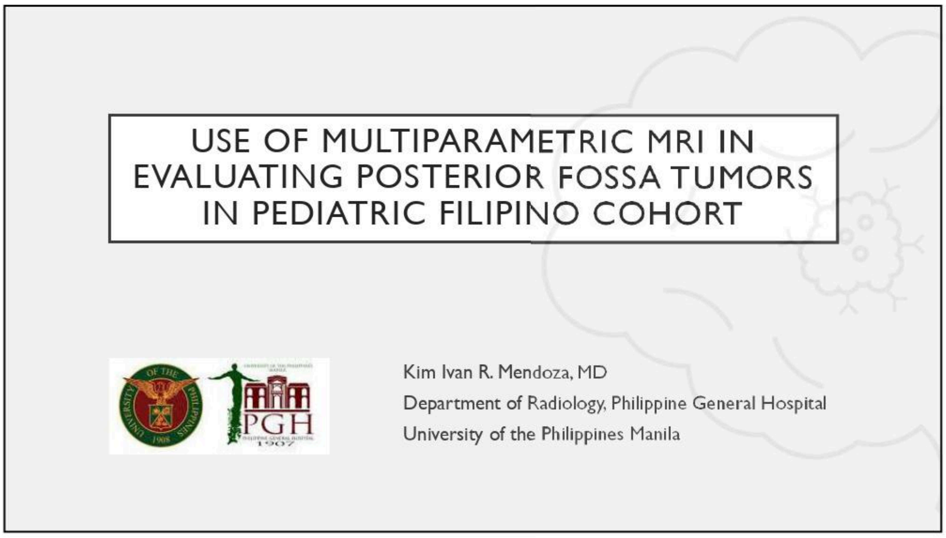

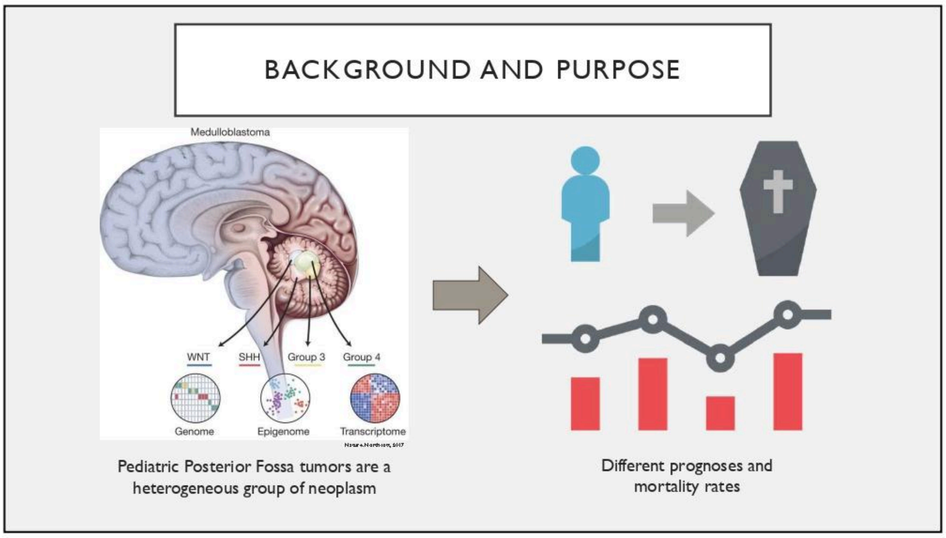

22nd Annual Scientific Meeting of Asian and Oceanic Society for Pediatric Radiology (AOSPR) 2024

BACKGROUND AND PURPOSE

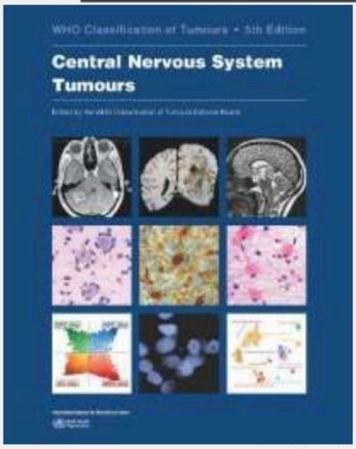

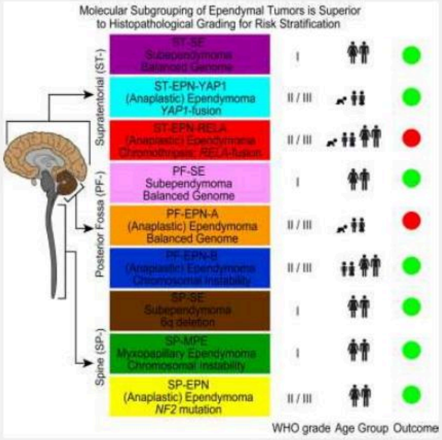

BACKGROUND AND PURPOSE

Challenges in low-middle-income countries like the Philippines

Difficult access to MRI; unrealized potential in LMICs

Resource-limited pathology departments

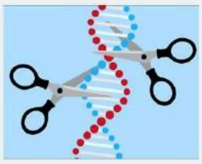

Poor access to genetic and molecular techniques

22nd Annual Scientific Meeting of Asian and Oceanic Society for Pediatric Radiology (AOSPR) 2024

MATERIALS AND METHODS

A database search of radiologically diagnosed posterior fossa tumors

January 2022 to February 2024

Less than 18 years old

Complete preoperative MRI scan

Histopathologically diagnosed posterior fossa medulloblastoma, pilocytic astrocytoma, ependymoma, and AT/RT

Preoperative MRI review and diagnosis of number-coded patients by three histopathologically blinded radiologists using Alves et al. MR-based numeric flowchart

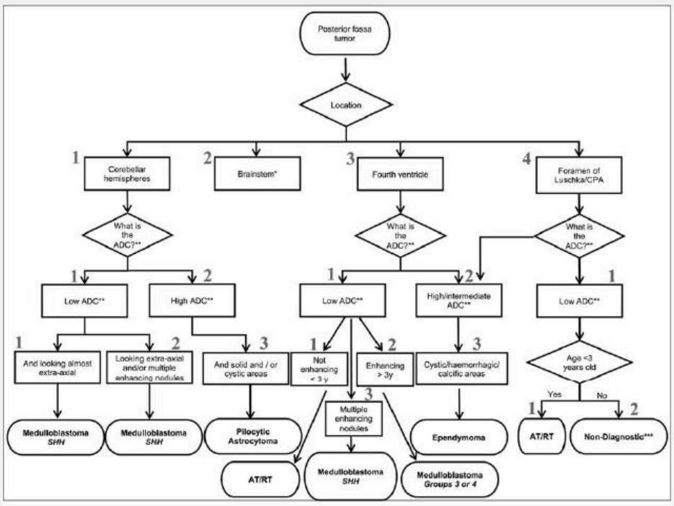

Figure 1. MR-based numeric flowchart from Alves et al 2021. Brainstem-arising tumors were excluded from the analysis and the ADC value/analysis was relative to gray matter.

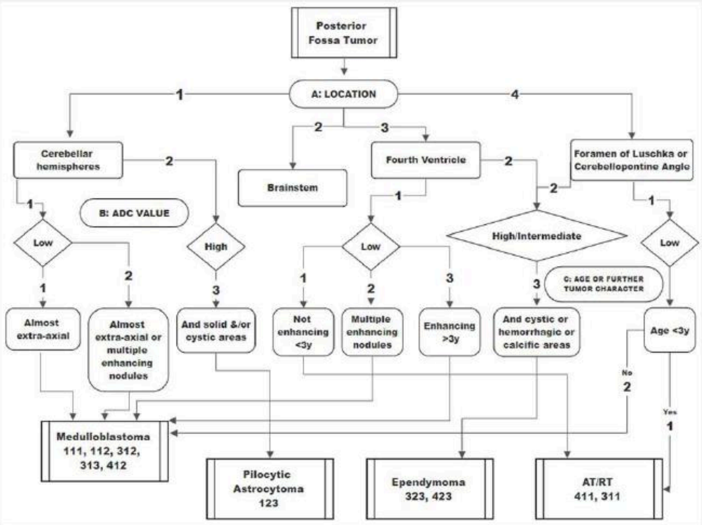

Figure 1. MR-based numeric flowchart adapted from Alves et al. Brainstem-arising tumors were excluded from the analysis and the ADC value/analysis was relative to gray matter.

RESULTS

Table 1. Clinicodemographic Characteristics of the Study Population

Characteristic	Overall	Medulloblastoma (N=25, 54.35%)	Pilocytic Astrocytoma (N=10, 21.74%)	Ependymoma (N=10, 21.74%)	AT/RT (N=1, 2.17%)
Age	7 (3–10)	7 (3–10)	8 (3–13)	5.5 (2–8)	0.67
Female	17 (36.96)	5 (20.00)	6 (60.00)	5 (50.00)	1 (100.00)
Location					
4th ventricle	29 (63.04)	21 (84.00)	2 (20.00)	5 (50.00)	1 (100.00)
Cerebellar vermis	3 (6.52)	0	3 (30.00)	0	0
Left CPA	4 (8.70)	1 (4.00)	0	3 (30.00)	0
Left Cerebellum	2 (4.35)	1 (4.00)	0	1 (10.00)	0
Right CPA	1 (2.17)	0	0	1 (10.00)	0
Right Cerebellum	7 (15.22)	2 (8.00)	5 (50.00)	0	0

Characteristic	Overall	Medulloblastoma (N=25, 54.35%)	Pilocytic Astrocytoma (N=10, 21.74%)	Ependymoma (N=10, 21.74%)	AT/RT (N=1, 2.17%)
T2 CHARACTER					
Cystic	8 (17.39)	0	8 (80.00)	0	0
Solid	10 (21.74)	10 (40.00)	0	0	0
Solid with hemorrhage	1 (2.17)	0	0	0	1 (100.00)
Solid with large cysts	13 (28.26)	7 (28.00)	2 (20.00)	4 (40.00)	0
Solid with large cysts & necrosis	1 (2.17)	0	0	1 (10.00)	0
Solid with necrosis	1 (2.17)	1 (4.00)	0	0	0
Solid with small cysts	12 (26.09)	7 (28.00)	0	5 (50.00)	0
Enhancement					
None	4 (8.70)	3 (12.00)	1 (10.00)	0	0
Present	28 (60.87)	14 (56.00)	6 (60.00)	8 (80.00)	0
Present (nodular)	14 (30.43)	8 (32.00)	3 (30.00)	2 (20.00)	1 (100.00)
ADC Value	750.625 (608–1086)	**633 (583.75–705.25)**	**1536.875 (1363.75–1786.25)**	1021.625 (873.75–1086)	639.5

Table 2. Statistical Analysis of MR-based numeric flowchart to discriminate posterior fossa tumors

Histopathologic diagnosis	TP	FP	FN	TN	Sn (%)	Sp (%)	PPV (%)	NPV (%)	LR+	LR-
Medulloblastoma	24	1	1	20	**96.00**	**95.24**	96.00	95.24	**20.16**	0.0420
Pilocytic Astrocytoma	7	1	3	35	70.00	**97.22**	87.50	92.11	**25.20**	0.3086
Ependymoma	9	4	1	32	90.00	88.89	69.23	**96.97**	8.10	0.1125
AT/RT	0	0	1	45	0	100.0	-	97.83	-	1.0000

22nd Annual Scientific Meeting of Asian and Oceanic Society for Pediatric Radiology (AOSPR) 2024

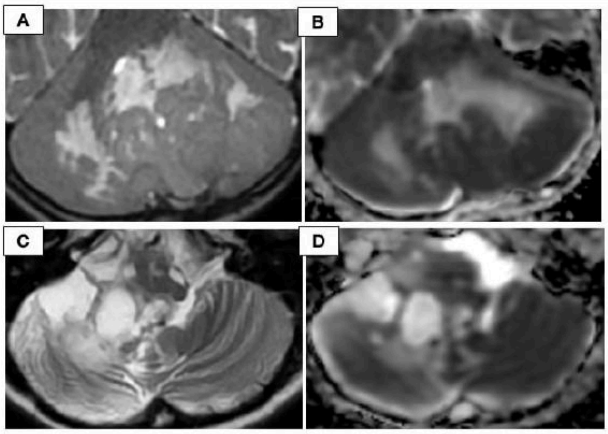

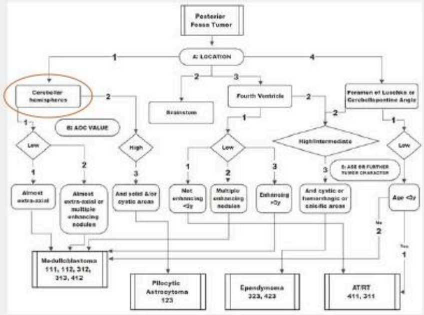

Figure 1. Differentials in pediatric posterior fossa masses centered in the cerebellar parenchyma. Axial T2WI (A) and ADC map (B) under pathway 1, with numeric flowchart of 112 suggesting medulloblastoma (histopathologically confirmed). Note the very low ADC values, presence of internal cysts, and large tumor infiltrating the left cerebellar parenchyma and vermis, all compatible with an embryonal tumor. Axial T2WI (C) and ADC map (D) under a similar pathway but with a numeric flowchart of 123, suggesting pilocytic astrocytoma (histopathologically confirmed). Notice the high ADC values and predominantly cystic appearance despite large tumor size and infiltration of the right cerebellar parenchyma.

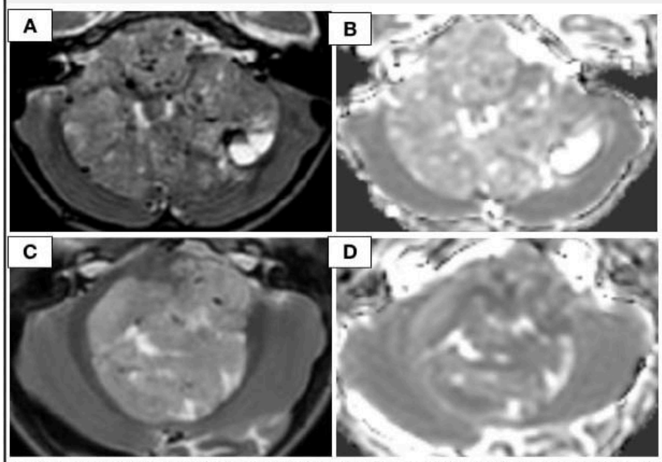

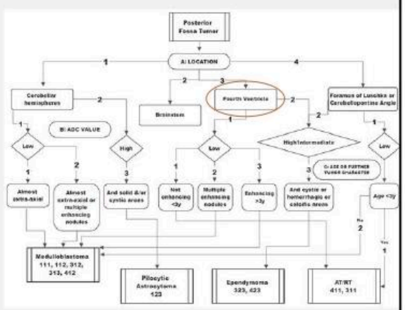

Figure 2. Differentials in pediatric posterior fossa masses centered in the fourth ventricle. Axial T2WI (A) and ADC map (B) under pathway 3, with numeric flowchart of 323 also suggesting ependymoma (histopathologically confirmed). Note the intermediate to high ADC despite large tumor size and internal vascularity, as well as presence of peripheral cysts. Axial T2WI (C) and ADC map (D) under a similar pathway but with numeric flowchart of 312, suggesting medulloblastoma (histopathologically confirmed). Notice the low ADC values and presence of internal cysts and vascularity, all suggestive of embryonal tumor.

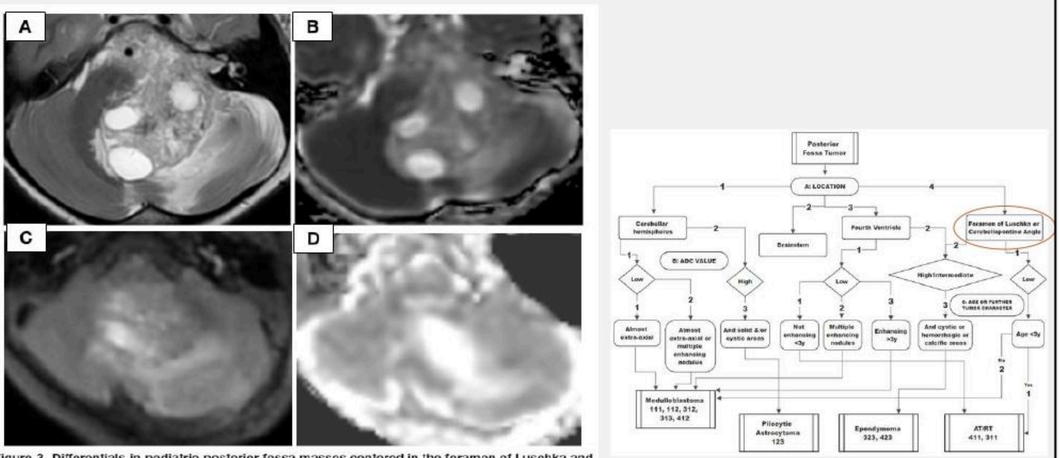

Figure 3. Differentials in pediatric posterior fossa masses centered in the foramen of Luschka and cerebellopontine angle. Axial T2WI (A) and ADC map (B) under pathway 4, with numeric flowchart of 423 suggesting ependymoma (histopathologically confirmed). Note the intermediate to high ADC and presence of cysts. Axial T2WI (C) and ADC map (D) under similar pathway but with numeric flowchart of 411 in a 5 month old child. In contrast to the other, note the low ADC values and similar presence of cysts. This only AT/RT patient was difficult to diagnose using the pathway as all radiologists centered the lesion in the fourth ventricle and noticed tumor enhancement (due to hemorrhage), thus calling a 312/313 sequence.

Table 3. Inter-rater Reliability of Pathways and Diagnoses Determined by the General Radiologist or the Resident Radiologist and the Neuroradiologist

Histopathologic diagnosis	According to numeric pathway			
	General radiologist		Resident radiologist	
	Agreement (%)	Kappa	Agreement (%)	Kappa
Overall	82.61	0.7881	80.43	0.7590
Medulloblastoma	76.00	0.6637	76.00	0.6495
Pilocytic Astrocytoma	90.00	0.7826	90.00	0.7826
Ependymoma	100.00	1.0000	80.00	0.6875

LIMITATIONS

- The study has some challenges, the main one being its **retrospective** nature. During image analysis, possible biases were controlled by **blinding** the MR interpreters with histopathologic diagnosis and **strict adherence** to the numeric-based flowchart.
- Another limitation of this study is its **small sample size** and **only one patient with AT/RT diagnosis**, which accounts for our confidence intervals and inability to calculate the diagnostic accuracy of pathway 311/411.
- Furthermore, the institution's **inability to classify medulloblastoma** into its **molecular subgroup** is a major limitation of this research, in contrast to the successful demonstration by the group of Alves et al.

IN SUMMARY

- This paper is the **first-largest cohort studying Filipino pediatric posterior fossa tumors**.
- **Medulloblastoma** is the most common pediatric posterior fossa tumor in our cohort
- The use of an MRI-based numeric pathway taking into account **age**, **location**, **tumor character**, and **ADC values** is diagnostically accurate in predicting histopathologic diagnosis, and possibly molecular subtype.
- This pathway is **easy to replicate** among neuroradiologists, general radiologists, and trainees, with substantial to near-perfect agreement.
- This stresses the importance of **adequate preoperative MRI evaluation** in our patients, as radiology can help **augment** the **resource-limited pathologic capabilities** of LMICs like the Philippines.

FURTHER DIRECTIONS

- **Collaboration** with other institutions can be done to produce a larger, more consistent analysis with an **increased sample size**, preferably using a **prospective** study design.
- Having a numeric flowchart that is validated and accurate can lead to the use of **radiogenomics** and **artificial intelligence applications**, now emerging fields in pediatric neuro-oncology.

REFERENCES

- Northcott PA, Buchhalter I, Morrissy AS, Hovestadt V, Weischenfeldt J, Ehrenberger T, et al. The whole-genome landscape of medulloblastoma subtypes. Nature. 2017 Jul;547(7663):311–7.
- Pajtler KW, Witt H, Sill M, Jones DT, Hovestadt V, Kratochwil F, Wani K, et. al. Molecular Classification of Ependymal Tumors across All CNS Compartments, Histopathological Grades, and Age Groups. Cancer Cell. 2015 May 11;27(5):728-43.
- Louis DN, Perry A, Wesseling P, Brat DJ, Cree IA, Figarella-Branger D, et al. The 2021 WHO Classification of Tumors of the Central Nervous System: a summary. Neuro-Oncology. 2021 Jun 29;23(8).
- Alves C a. PF, Löbel U, Martin-Saavedra JS, Toescu S, Tsunemi MH, Teixeira SR, et al. A Diagnostic Algorithm for Posterior Fossa Tumors in Children: A Validation Study. AJNR American journal of neuroradiology. 2021 May 1;42(5):961–8.
- Hanzlik E, Woodrome SE, Abdel-Baki M, Geller TJ, Elbabaa SK. A systematic review of neuropsychological outcomes following posterior fossa tumor surgery in children. Child's Nervous System. 2015 Sep 9;31(10):1869–75.
- Orduña P, Cheryl Anne Lubaton-Sacro. Factors associated with delayed diagnosis among Filipino pediatric brain tumor patients: a retrospective review. CNS oncology. 2022 Jun 9;11(3).

THANK YOU FOR YOUR KIND ATTENTION

For the Filipino children and every kid in the world battling and standing tall against all odds.

Confidence level	95%
Population Propotion	0.42
Marginal Error	0.08
Population Size	61
Alpha divided by 2	0.025
Z-score	1.959963985
Numerator	146.2155264
Denominator	3.396975842
n (sample)	**43.0428514**

Risk of Acute Kidney Injury After Contrast-enhanced MRI Examinations In A Pediatric Population

Hana Jeong[1], Pyeong Hwa Kim[1], Ah Young Jung[1], Jin Seong Lee[1], Young Ah Cho[1], Chong Hyun Suh[1], Jiwon Jung[2], Hee Mang Yoon[1]

1 Department of Radiology and Research Institute of Radiology, University of Ulsan College of Medicine, Republic of Korea
2 Department of Pediatrics, Asan Medical Center, University of Ulsan College of Medicine, Seoul, Republic of Korea

22nd Annual Scientific Meeting of Asian and Oceanic Society for Pediatric Radiology (AOSPR) 2024

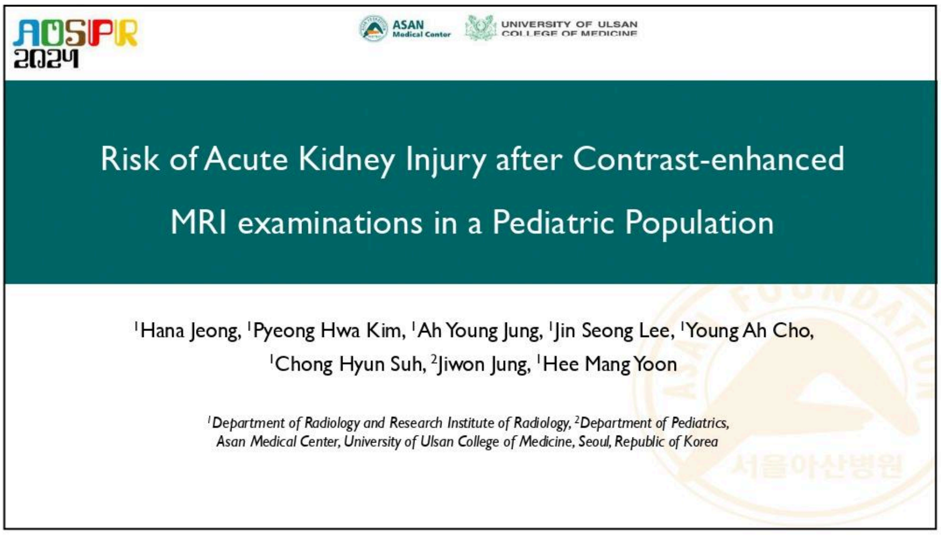

1

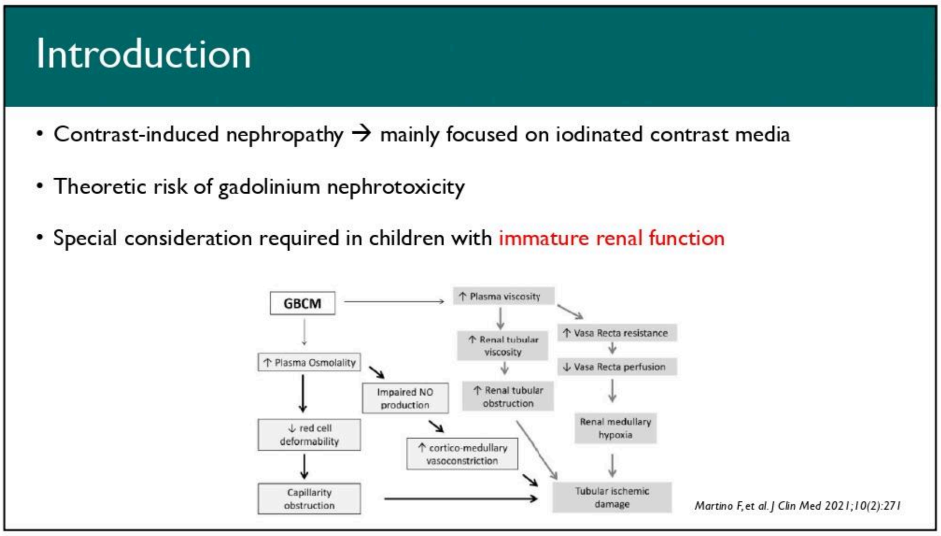

2

Purpose

To investigate the associations between GBCA administration and the occurrence of AKI in pediatric patients, and to determine the risks associated with AKI

3

Materials and Methods

4

Patients

- Single center, retrospective cohort study
- Consecutive pediatric patients (≤ 18 years) who underwent contrast-enhanced or unenhanced MRI between January 2015 ~ June 2021
- Exclusion
  - Unavailable height, weight, or serum creatinine within 3 months before MRI
  - Unavailable serum creatinine within 2 days after MRI
  - GBCA not administered intravenously (e.g., MR lymphangiography)
  - Additional MRI examinations obtained in one sitting (e.g., consecutive brain → spine MRI in one slot)
    - Only the prior MRI examination included

5

Outcomes

Primary outcome

Occurrence of AKI

Enhanced vs. unenhanced MRI

- Serum creatinine ≥ 0.3 mg/dL or 50% within 48 hours after MRI

K-DIGO guideline (Nephron Clin Pract 2012;120:c179-84)

Variables for propensity score estimation

- Age
- Examination type (CNS vs. non-CNS)
- Body mass index
- Calculated eGFR (bedside Schwartz calculation)
- CKD stage
- Diabetes mellitus
- Cardiovascular disease

Statistical analysis

① Per-examination basis Multivariable logistic regression analysis using generalized estimating equation (GEE)

② Propensity score matching (PSM)

③ Inverse probability of treatment weighting (IPTW) analysis

6

Statistical analysis

- Multivariable logistic regression using GEE to explore factors associated with AKI after MRI
- Propensity score analysis
  - Hosmer-Lemeshow test → discrimination for propensity score model
  - C-statistic → calibration for propensity score model
  - Standardized mean difference (SMD) > 0.1 → considered as imbalanced
- Subgroup analysis (age, sex, CKD stage, diabetes mellitus, cardiovascular disease)

7

Results

8

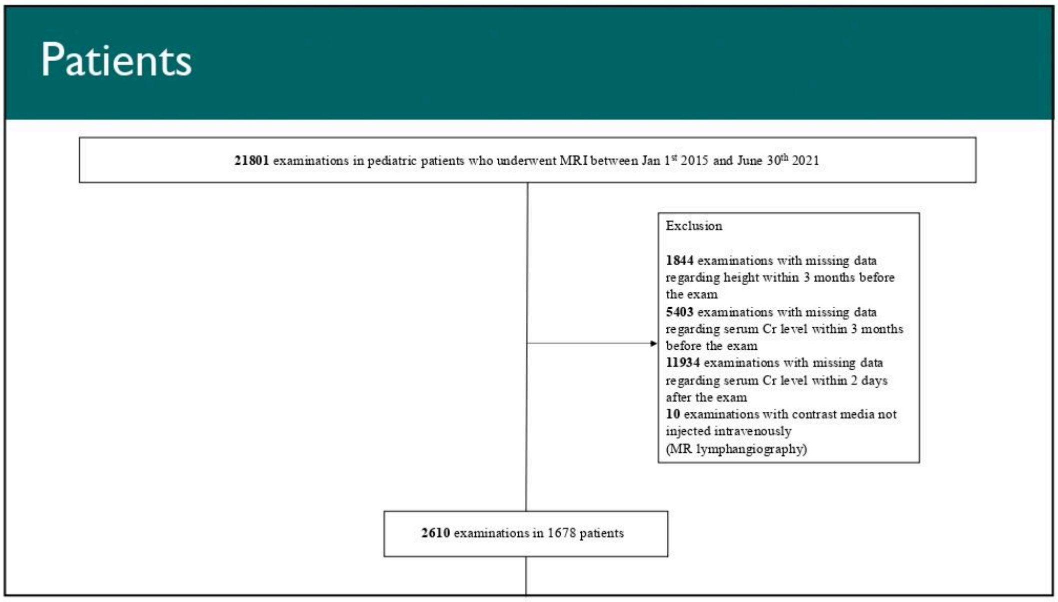
Patients
21801 examinations in pediatric patients who underwent MRI between Jan 1st 2015 and June 30th 2021
Exclusion
1844 examinations with missing data regarding height within 3 months before the exam
5403 examinations with missing data regarding serum Cr level within 3 months before the exam
11934 examinations with missing data regarding serum Cr level within 2 days after the exam
10 examinations with contrast media not injected intravenously (MR lymphangiography)
2610 examinations in 1678 patients

9

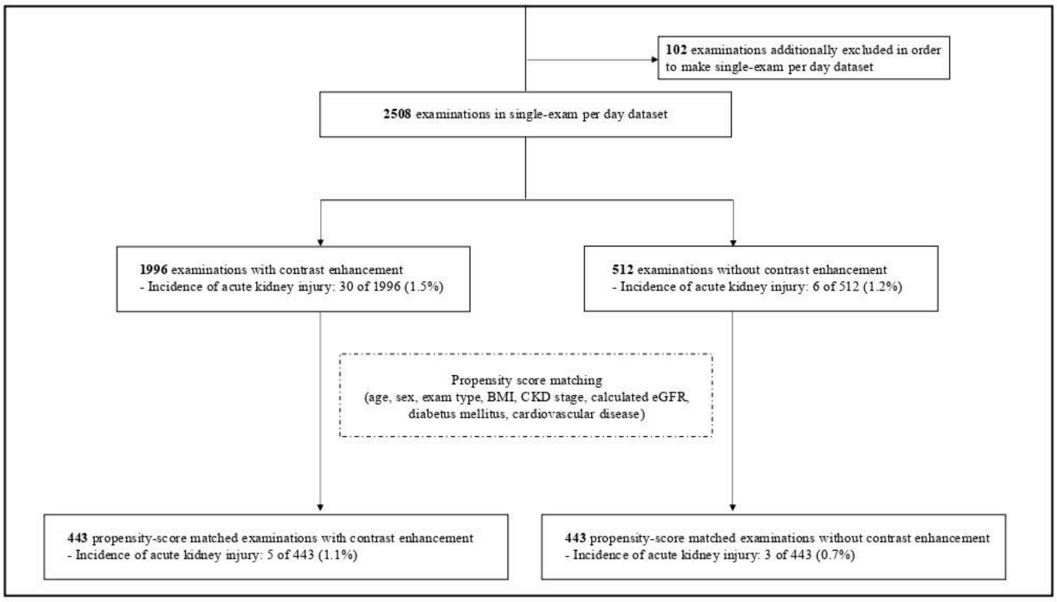
102 examinations additionally excluded in order to make single-exam per day dataset
2508 examinations in single-exam per day dataset
1996 examinations with contrast enhancement
- Incidence of acute kidney injury: 30 of 1996 (1.5%)
512 examinations without contrast enhancement
- Incidence of acute kidney injury: 6 of 512 (1.2%)
Propensity score matching
(age, sex, exam type, BMI, CKD stage, calculated eGFR, diabetus mellitus, cardiovascular disease)
443 propensity-score matched examinations with contrast enhancement
- Incidence of acute kidney injury: 5 of 443 (1.1%)
443 propensity-score matched examinations without contrast enhancement
- Incidence of acute kidney injury: 3 of 443 (0.7%)

10

Baseline characteristics

	Total set (n=2508)			Propensity score matched set (n=886)			IPTW set (n=3378)		
Characteristic	Noncontrast group (n=512)	Contrast group (n=1996)	SMD	Noncontrast group (n=443)	Contrast group (n=443)	SMD	Noncontrast group (n=1706)	Contrast group (n=1672)	SMD
Mean age, years	9.0 ± 6.9	9.3 ± 6.2	0.06	9.0 ± 6.8	9.3 ± 6.3	0.05	9.2 ± 6.7	8.8 ± 6.4	0.06
Sex			0.15			0.01			0.08
Boys	241 (47.1)	1087 (54.5)		202 (45.6)	205 (46.3)		949 (55.6)	863 (51.6)	
Girls	271 (52.9)	909 (45.5)		241 (54.4)	238 (53.7)		757 (44.4)	809 (48.4)	
Exam type			0.38			0.12			0.06
Non-CNS	77 (15.0)	616 (30.9)		67 (15.1)	87 (19.6)		478 (28.0)	512 (30.6)	
CNS	435 (85.0)	1380 (69.1)		376 (84.9)	356 (80.4)		1228 (72.0)	1160 (69.4)	
Body mass index, kg/m^2	18.17 (5.2)	18.56 (4.6)	0.08	18.2 (5.1)	18.4 (5.0)	0.05	18.8 (5.4)	18.4 (4.7)	0.08
CKD stage			0.38			0.15			0.06
1	333 (65.0)	1594 (79.9)		297 (67.0)	303 (68.4)		1228 (72.0)	1230 (73.6)	
2	101 (19.7)	278 (13.9)		86 (19.4)	94 (21.2)		315 (18.5)	282 (16.9)	
3	40 (7.8)	88 (4.4)		34 (7.7)	28 (6.3)		107 (6.3)	103 (6.2)	
4	24 (4.7)	29 (1.5)		18 (4.1)	16 (3.6)		39 (2.3)	46 (2.7)	
5	14 (2.7)	7 (0.4)		8 (1.8)	2 (0.5)		17 (1.0)	11 (0.7)	
Calculated eGFR, $mL/min/1.73m^2$	100.3 ± 44.4	123.8 ± 48.6	0.51	100.9 ± 41.2	105.0 ± 39.8	0.10	116.8 ± 61.8	111.9 ± 42.9	0.09
Diabetes mellitus	7 (1.4)	41 (2.1)	0.05	5 (1.1)	7 (1.6)	0.04	32 (1.9)	27 (1.6)	0.02
Cardiovascular disease	33 (6.4)	162 (8.1)	0.06	26 (5.9)	23 (5.2)	0.03	130 (7.6)	111 (6.7)	0.04

Noncontrast group showed

- CNS (e.g., brain or spine) exam↑
- Renal insufficiency↑

→ Imbalanced in PSM, but balanced in IPTW

Acceptable

Calibration

Hosmer-Lemeshow
P=0.40 (>0.05)

Discrimination

C-statistic=0.689

11

Risk of AKI

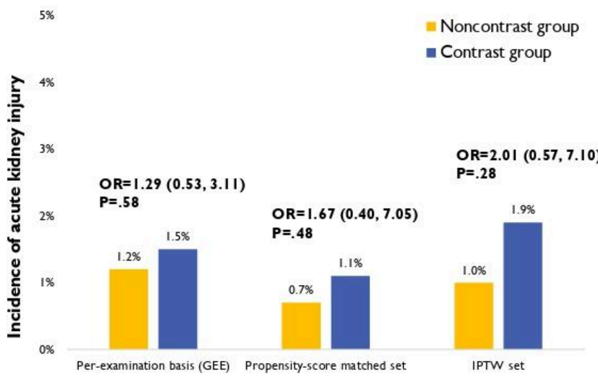

No significant difference of AKI

Enhanced vs. unenhanced MR

12

Regression and subgroup analysis

Factors associated with AKI

Variable	OR (95% CI)	P-value
Age	0.94 (0.89–1.00)	0.051
Sex	Eliminated	
Examination type	Eliminated	
BMI	Eliminated	
CKD stage		
1	Reference category	
2	0.37 (0.09–1.54)	0.17
3	0.38 (0.05–3.00)	0.36
4	0.94 (0.12–7.29)	0.95
5	10.66 (3.15–36.09)	<0.001
Calculated eGFR	Eliminated	
Diabetes mellitus	3.63 (0.74–17.97)	0.11
Cardiovascular disease	Eliminated	

Subgroup analysis

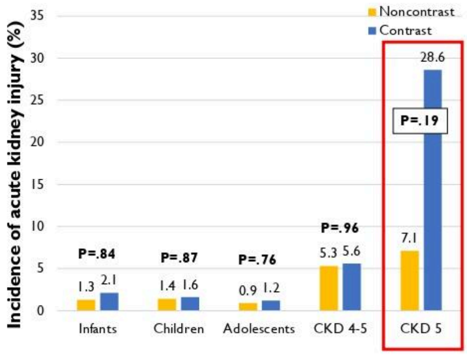

13

Limitation

- Sample size (especially neonates, CKD stage 5)
- Exclusively used gadoterate meglumine (97%)
- Urine output (one of AKI criteria) not considered
- Confounding variables (e.g., nephrotoxic drug or sepsis) not fully considered

14

Conclusion

- The incidence rate of acute kidney injury following contrast-enhanced MRI examinations was similar to that following unenhanced MRI examinations.

- Although there was no interaction between CKD stage and GBCA, numerically higher incidence of AKI in the contrast group with CKD stage 5 warrants careful interpretation.

15

Thank you for the attention!

Pyeong Hwa Kim, MD, PhD
phkim@amc.seoul.kr

Assistant professor

Department of Radiology and Research Institute of Radiology, Asan Medical Center, University of Ulsan College of Medicine, Korea

16